White Rose Research Online
eprints@whiterose.ac.uk
https://eprints.whiterose.ac.uk
Universities of Leeds, Sheffield and York

Deposited via The University of Sheffield.

White Rose Research Online URL for this paper:
https://eprints.whiterose.ac.uk/id/eprint/207900/

Version: Accepted Version

Article:

Wymeersch, F.J., Wilson, V. and Tsakiridis, A. (2021) Understanding axial progenitor biology in vivo and in vitro. Development, 148 (4). dev180612. ISSN: 0950-1991

https://doi.org/10.1242/dev.180612

© 2021 Published by The Company of Biologists Ltd. This is an author-produced version of a paper subsequently published in Development. Uploaded in accordance with the publisher's self-archiving policy.

Reuse
Items deposited in White Rose Research Online are protected by copyright, with all rights reserved unless indicated otherwise. They may be downloaded and/or printed for private study, or other acts as permitted by national copyright laws. The publisher or other rights holders may allow further reproduction and re-use of the full text version. This is indicated by the licence information on the White Rose Research Online record for the item.

Takedown
If you consider content in White Rose Research Online to be in breach of UK law, please notify us by emailing eprints@whiterose.ac.uk including the URL of the record and the reason for the withdrawal request.

UNIVERSITY OF LEEDS
University of Sheffield
UNIVERSITY of York

Understanding axial progenitor biology *in vivo* and *in vitro*

Authors: Filip J. Wymeersch[1], Valerie Wilson[2], Anestis Tsakiridis[3,4]

[1]Laboratory for Human Organogenesis, RIKEN Center for Biosystems Dynamics Research,
2-2-3 Minatojima-minamimachi, Chuo-ku, Kobe, 650-0047, Japan.
[2]Centre for Regenerative Medicine, Institute for Stem Cell Research, School of Biological
Sciences, University of Edinburgh, 5 Little France Drive, Edinburgh EH16 4UU United
Kingdom.
[3]Centre for Stem Cell Biology, Department of Biomedical Science, The University of
Sheffield, Western Bank, Sheffield S10 2TN United Kingdom.
[4]Neuroscience Institute, The University of Sheffield, Western Bank, Sheffield, S10 2TN
United Kingdom.

Keywords: axis elongation, gastrulation, neuromesodermal progenitors, primitive streak, tail bud, pluripotent stem cells

Summary

The generation of the components that make up the embryonic body axis, such as the spinal cord and vertebral column, takes place in an anterior to posterior (head-to-tail) direction. This process is driven by the coordinated production of various cell types from a pool of posteriorly-located axial progenitors. Here, we review the key features of this process and the biology of axial progenitors, including neuromesodermal progenitors (NMPs), the common precursors of the spinal cord and trunk musculature. We discuss recent developments in the *in vitro* production of axial progenitors and their potential implications in disease modelling and regenerative medicine.

Introduction

Lineage specification in the early vertebrate embryo is initiated during gastrulation (see Glossary, **Box 1)**, which involves the formation of the three germ layers (ectoderm, mesoderm and endoderm) via cell ingression and epithelial-to-mesenchymal transition (EMT) from a localised region of the primitive, pluripotent epithelium. This region is known as the primitive streak (PS) in amniotes. Following gastrulation, embryonic anteroposterior (A-P) axis elongation lasts until the end of somite production (somitogenesis). In all vertebrates, the arrangement of the axial tissues depends on a structure present during gastrulation known as the organiser (reviewed in (Anderson and Stern, 2016; Martinez Arias and Steventon, 2018). The organiser itself gives rise to midline axial tissues such as the notochord and ventral neural tube (the progenitor of the floor plate). Signals from the organiser also pattern the surrounding cells such that those closer to the organiser differentiate as more medial (midline) structures. In the ectoderm, the medial-to-lateral axis is made up of successively more dorsally-fated neural tissues flanked by surface ectoderm. Meanwhile, mesoderm precursors produce the paraxial, intermediate and lateral plate/ventral mesoderm (see Glossary, Box 1; **Fig. 1**). Despite a reorganisation of cells around the organiser during axial elongation to form the growing posterior (or caudal) end of the embryo termed the tail bud (**Fig. 1**), the progenitors for further axial elongation remain in this caudal location until the end of axis elongation. These progenitors generate sequentially more posterior neural and mesodermal components of the axis, starting from around the base of the future hindbrain, and ending at the tip of the tail. Collectively known as axial progenitors, they are responsible for producing a large fraction of the spinal cord and musculoskeleton, the notochord, as well as the body wall and mesodermal organs, such as the kidneys and gonads (**Fig. 1**).

Research in the last two decades has clarified the number of progenitor types, their locations, fate and potency (see Glossary, Box 1), and how construction of the A-P axis varies between vertebrates. Moreover, recent pluripotent stem cell (PSC)-based models have provided novel insights into various aspects of this process. The link between PSC-based models and disease modelling/regenerative medicine applications has stimulated a wider interest in axial progenitor biology, coming from a diverse range of disciplines and perspectives (**Box 2**). In this Review, we provide an overview of the field, focusing particularly on the progenitors of the spinal cord and trunk skeletal muscle/vertebral column and their role in the conceptual development of novel PSC differentiation strategies.

Axial progenitors *in vivo*

Evidence for multi-fated axial progenitors and their locations

Anatomical studies, grafting and lineage-tracing experiments have provided compelling evidence about the existence of multipotent axial progenitors, their location and contribution to different tissues. First, we discuss data from amniotes, where several key advances have been made, and compare these with data from anamniotes.

Amniotes

Lineage tracing in gastrulation-stage chick embryos provided some of the earliest indications that multi-fated axial progenitors are located within defined PS regions. Selleck and Stern showed that descendants of single node cells could be found in more than one germ layer, specifically the neural tube and notochord. Moreover, the descendants of these labelled cells were retained in the progenitor region, leading to the hypothesis that some cells in the node area exhibit stem cell-like properties (Selleck and Stern, 1991). This has been further supported by experiments in mouse embryos, showing that labelling of individual node/streak cells at various gastrulation stages (Forlani et al., 2003; Lawson et al., 1991), or groups of node cells in early somite-stage embryos (Wilson and Beddington, 1996), produces descendants in both the differentiated notochord and the node itself, even after relatively long periods of axis elongation (48 hours, forming half (~30) of the total somite number).

Retrospective clonal analyses in the myotome (see Glossary, Box 1) (Nicolas et al., 1996), neural tube (Mathis and Nicolas, 2000), or in the entire embryo (Tzouanacou et al., 2009) each produced clones that contributed to tissues over large anteroposterior distances. These clones contributed from a variable anterior point as far as the posterior end, indicating an increased probability of recombination in a long-lived progenitor over time. This suggests a continuing stem cell-like progenitor at the posterior end of the embryo. Clones contributing to both neural and (principally paraxial, i.e. somitic) mesodermal tissues, but no other tissue types, indicate a dual-fated neuromesodermal progenitor (NMP). However, retrospective clonal analysis infers the properties of a progenitor from its descendants and requires prospective analyses to identify potential locations for these progenitors.

Prospective fate mapping via dye injection or grafting of small tissue pieces in the PS area of cultured mouse embryos has identified two such regions of neuromesodermal (NM) fate: the node-streak border (NSB) and the anterior caudal lateral epiblast (CLE) on either side of the PS (**Fig. 2A**). These two areas differ in their contribution to the two lineages: the NSB gives rise to medially-located cells in the somites and the ventral neurectoderm, while the CLE produces more lateral somitic cells and mainly lateral neurectoderm (Cambray and Wilson, 2007; Mugele, 2018; Wymeersch et al., 2016). Only the dorsal part of the NSB contributes to both neurectoderm and mesoderm. By contrast, the ventral part of the NSB contains notochord progenitors (NotoPs) (Cambray and Wilson, 2007; Kinder et al., 1999; Wilson and Beddington, 1996) (**Fig. 2A-B**). Interestingly, the relative quiescence of the ventral node has been suggested to indicate a stem cell-like character of these progenitors (Bellomo et al., 1996; Ukita et al., 2009). However, the ventral node cells at the NSB itself, termed the ‘crown’, are more proliferative (Wymeersch et al., 2019). At embryonic day (E) 8.5, other areas of distinct fate include the anterior half of the PS, which harbours predominantly paraxial mesoderm-fated progenitors. In contrast, the posterior-most PS and CLE contains progenitors of lateral plate mesoderm (termed lateral and paraxial mesoderm progenitors or LPMPs, after their lineage potential), which exit the PS as the tail forms (**Fig. 2A**) (Cambray and Wilson, 2007; Kinder et al., 1999; Mugele, 2018; Wymeersch et al., 2016). During trunk-to-tail transition, the NSB gives rise to a region within the tail bud called the chordoneural hinge (CNH; see Glossary, Box 1) (Cambray and Wilson, 2002; Wilson and Beddington, 1996). This region also contains axial progenitors with dual NM fate (Catala et al., 1995; McGrew et al., 2008; Wilson and Beddington, 1996). The CNH itself comprises the notochord end, derived mainly from the ventral NSB cells (Wymeersch et al., 2019) and overlying epithelial tissue continuous with the neurectoderm, where NMPs are likely to reside (Box 3; **Fig. 2C**) (Cambray and Wilson, 2002).

More recent work has shown that while NSB cells contribute fairly equally to both neural and mesodermal derivatives, the fate of NM-potent cells in the CLE is dependent on their exact location in the epiblast layer: anterior and lateral cells contribute largely to neural tube, while posterior and medial cells contribute more to mesodermal tissues (Wymeersch et al., 2016) (**Fig. 2D**). Furthermore, the observation that the majority of the dorsal CNH derives from NSB cells, while only a minor proportion of cells derive from the CLE adds further diversity to NMP fates (Cambray and Wilson, 2007; Catala et al., 1995). This suggests that NMP subpopulations are biased towards neural or mesodermal differentiation outcomes, and towards long or short-term contribution to the axis depending on their physical location. Alternatively, different NMP subtypes might occupy these separate locations (see 'fate versus potency' section below).

The presence of dual NM-fated cells in posterior locations equivalent to those in mouse has been demonstrated during chick embryonic axis elongation (Brown and Storey, 2000; Guillot, 2020; Iimura et al., 2007; McGrew et al., 2008; Wood, 2019) (**Fig. 3A-B**). More recently, the early origin and later location of individual dual-fated cells has been described using live imaging (Guillot, 2020; Wood, 2019), which revealed that cells that produce neural and mesodermal descendants lie at the interface between cells of purely neural or mesodermal fate. These NM progenitors form an arc around the node at the end of gastrulation, which gradually extends posteriorly to form an inverted 'U' shape, similar to that seen in mouse (**Fig. 2A; 3A**).

Anamniotes

While evidence in chick and mouse supports the existence of NM-fated progenitors that contribute over large stretches of posterior axis, NMP contribution to anamniote axial elongation is unclear. Work in the early 2000s in the *Xenopus* tail showed that multi-fated descendants were observed after focal labelling earlier-stage tail bud (Davis and Kirschner, 2000). However, the photoactivation method employed in that study labelled small groups of cells, rather than individual ones. Careful anatomical studies in frog identified a region present after gastrulation in the elongating axis, where the ventral neural tube was continuous with the underlying notochord. This region was termed the chordoneural hinge (CNH) and is delimited posteriorly by a small continuous cavity between the neural tube and the gut, termed the neurenteric canal (see Glossary, Box 1; **Fig. 3C-D**). Interestingly, although this cavity is absent in the mouse, it is present during gastrulation in many other species, including human (Rulle et al., 2018) (**Fig. 3G**). This indicates a well-conserved discontinuity between the dorsal blastopore lip and CNH on the one hand, and the lateral part of the blastopore and posterior wall of the tail bud on the other (**Fig. 3C-D**). Lineage tracing further showed that the CNH is derived from the organiser and is fated for the midline (ventral neural tube and notochord), whereas the cells on the posterior side of the neurenteric canal produce paraxial mesoderm (Gont et al., 1993), as does the PS (Beck and Slack, 1998; Beck and Slack, 1999; Tucker and Slack, 1995). The lineage continuity of cells from the late blastopore to the CNH suggests that the organisation of axial progenitors and their progression to the tail bud is similar to that in amniotes (Gont et al., 1993). However, the *Xenopus* tail-forming region includes a large section of tissue anterior to the blastopore as trunk cells are incorporated into the tail by anterior displacement of the anus during body extension (Tucker and Slack, 1995). In contrast, recent grafting in the axolotl embryo has shown that the posterior third of the trunk and the entire tail is derived from a region of the posterior neural plate (which co-expresses *Sox2* and *Brachyury*, see below), suggesting that the extent to which tissue rearrangement contributes to axis elongation varies between species (Taniguchi et al., 2017).

In the zebrafish, single-cell fate mapping has shown that a region of overlapping neurectoderm and mesoderm fate exists near the organiser at early gastrulation stages (Kimmel et al., 1990). In contrast, single-cell injections by Kanki and Ho produced no multi-fated progenitors during later tail development (Kanki and Ho, 1997). More recently, Martin and Kimelman confirmed that – consistent with amniotes – zebrafish embryos harbour bipotent axial progenitors throughout posterior body formation, because mesoderm-fated cells can switch fate and give rise to neural tissue upon depletion of β-catenin signalling (Martin and Kimelman, 2012) (**Fig. 3E-F**). Since the presence of bipotent cells does not necessarily imply dual fate, these findings can be reconciled with those of Kanki and Ho if the majority of cells with neuromesodermal potency do not actually give rise to both neural and mesodermal lineages. Indeed, single-cell tracking in the zebrafish tail bud has shown that only a minority of cells exhibit both fates (Attardi et al., 2018) suggesting that, despite a localised region of NM fate, the number of individual dual-fated cells might be low in fish. In fact, NM contributions are restricted to the last seven to nine tail segments (Attardi et al., 2018) with the largest volumetric increase of trunk tissue in fish originating from the displacement of lateral cells to the posterior, instead of being laid down by the tail bud (Steventon et al., 2016) (**Fig. 3E-F**). Thus contributions of NM-fated axial progenitors in fish (and possibly also in frog) appear more limited to the posterior-most regions of the axis than those in chick and mouse, and instead the majority of axis elongation relies more on convergence and extension of pre-existing neural and mesodermal tissue formed during gastrulation.

Further volumetric comparisons between lamprey, dogfish and mouse embryos have revealed that the latter two species, which have relatively long anteroposterior axes, initially increase the volume of their unsegmented mesoderm (producing anterior somites), after which it decreases during later elongation to produce the posterior somites (Steventon et al., 2016). This volumetric expansion and contraction has also been observed for a number of organisms, including chicken, mouse and snake (Gomez et al., 2008). Interestingly, in the mouse embryo, the number of putative NMPs shows a similar trajectory of expansion and contraction during elongation (Wymeersch et al., 2016) and a reorganisation in the progenitor pool around tail bud formation (Tzouanacou et al., 2009), which are likely to precede changes in axial tissue volume. While recent studies have elucidated some of the mechanisms underlying trunk-to-tail transition and their effects on axial progenitors (see below), it remains to be investigated how axial progenitor numbers and dynamics shape diverse body plans during elongation across different species.

Axial progenitor fate vs potency: Spatial environment

As mentioned above, in the NM-fated zone of the early somitogenesis stage mouse (E8.0-E8.5), the anterior/lateral and posterior/medial regions of the CLE tend to produce neurectoderm and mesoderm fates, respectively (Wymeersch et al., 2016). As in fish, this suggests that NM fate may not be exhibited by all cells with NM potency. Consistent with this idea, heterotopic grafts of these differentially-fated regions have shown that it is the environment, rather than their level of commitment, that dictates these differential fates (Wymeersch et al., 2016). Indeed, NMPs can also form exclusively lateral plate mesoderm upon transplantation to the posterior PS, although they do not generally exhibit this fate in undisturbed embryos (Cambray and Wilson, 2007; Row et al., 2018; Tzouanacou et al., 2009; Wymeersch et al., 2016). Wider potency than fate appears to be a general property of the region surrounding the PS, since lateral mesoderm-fated PS cells can form paraxial mesoderm upon transplantation to paraxial mesoderm-fated regions of the PS (therefore termed LPMPs) (Wymeersch et al., 2016). Similar environment-driven cell fate changes have been also reported in chick (Wood, 2019), suggesting that extrinsically-imposed neural or mesodermal differentiation on NM potent cells is essential to ensure correctly balanced production of neural and mesodermal subtypes during axis elongation. Despite this developmental plasticity, kidney capsule grafts have shown that cells in NM-fated regions are restricted to neural and mesodermal fates from the beginning of somitogenesis until at least E10.5 (Osorno et al., 2012; Wymeersch et al., 2016). In contrast, LPMPs do not give rise to neurectoderm in kidney capsule assays. Thus, the fate of NMPs and LPMPs is restricted both by their location and by their intrinsic potential to differentiate.

Axial progenitor fate vs potency: Temporal environment

Surprisingly, the differentiation of axial progenitors is not only affected by their spatial but also their temporal environment. CNH cells contribute to anterior neurectoderm and paraxial mesoderm when grafted heterochronically into the E8.5 NSB (Cambray and Wilson, 2002). Indeed, NMP descendants in the tail bud mesoderm up to E13.5 also demonstrate this property (Tam and Tan, 1992). Furthermore, NMPs can be serially passaged from CNH to NSB through multiple generations of embryos and – at least in chick – descendants of these 'late' NMPs grafted to early stage embryos, can adopt the A-P identity of the host environment (Cambray and Wilson, 2002; McGrew et al., 2008). The adaptability of NMPs to temporally unmatched environments, together with the finding that their transcriptome changes dramatically over time (Wymeersch et al., 2019), suggest that the temporal NMP transcriptional state is set (at least in part) by extrinsic signals. Nevertheless, cells grafted heterochronically integrate less efficiently into host tissues than isochronic grafts (whether heterotopic or homotopic), suggesting that this temporal resetting may be less efficient than their acutely sensitive response to spatial cues.

Genes and signals driving axial progenitor cell fate decisions

Despite extensive transcriptome analysis, mainly of amniote embryos at both the single-cell and bulk-population level (de Lemos, 2019; Gouti et al., 2017; Guillot, 2020; Koch et al., 2017; Olivera-Martinez et al., 2014; Wymeersch et al., 2019), no unique, exclusive markers that detect NMPs at all stages have been identified to date. In mice, the best readout of NM bipotency appears to be the co-expression of definitive neural and mesodermal genes, such as the transcription factors Sox2 and Brachyury (T) (Henrique et al., 2015; Tsakiridis et al., 2014). T^+Sox2^+ double positive cells emerge at the end of gastrulation at E7.5 and persist in NM-potent regions until axis elongation ends at E13.5 (Wymeersch et al., 2016). T^+Sox2^+ cells have been identified in analogous regions of the developing tail bud in zebrafish, chick and human embryos (Guillot, 2020; Martin and Kimelman, 2012; Olivera-Martinez et al., 2012) (**Fig. 3, 4**). Lineage tracing experiments in mice have also confirmed that posterior neurectoderm cells in the spinal cord are derived from T^+ progenitors (Anderson et al., 2013; Mugele, 2018; Perantoni et al., 2005). However, more recent studies have raised doubts about the extent of the contribution of T^+ and $Sox2^+$ cells into the neural tube and paraxial mesoderm, respectively (Mugele, 2018; Serizawa et al., 2019). These findings may reflect differences in the efficiency of the recombinase systems employed and their relative dependencies on the activity levels of the promoters driving their expression (Araki et al., 1997). Therefore, further experiments are required to clarify the discrepancy with published lineage tracing studies and expression data on NM-potent regions.

In addition to *T* and *Sox2* co-expression, transcriptome analyses and lineage tracing experiments have revealed a number of other posteriorly-expressed genes, such as *Nkx1-2*, *Cdx2*, *Epha1, Tbx6* and Hox family members, that mark NMPs or NMP subsets in the mouse (Garriock et al., 2015; Javali et al., 2017; Rodrigo Albors et al., 2018) (**Table 1, 2; Fig. 5A**).

These markers also include components of various signalling pathways, predominantly Wnt and Fgf. Loss-of-function studies have demonstrated that many of these genes (e.g. *T*, *Cdx2* and trunk Hox genes) are also key regulators of NMP ontogeny (**Table 1, 2**) acting downstream of Wnt and Fgf signalling inputs to control both mesoderm production and progenitor maintenance (Ciruna and Rossant, 2001; Takemoto et al., 2011; Wymeersch et al., 2016; Yamaguchi et al., 1999). Conversely, Nodal and Shh components are found in notochord precursor regions in the node, and BMP-associated transcripts are enriched in LPMPs in the posterior PS (**Table 2; Fig. 5A**).

Transcriptome analysis has shown that mouse NMPs at early (E8.0–E8.5) and later (tail bud) stages of axial elongation are substantially distinct, despite their shared ability to produce neurectoderm and mesoderm (Dias et al., 2020; Gouti et al., 2017; Wymeersch et al., 2019). Interestingly, components of the Wnt, Fgf and Notch signalling pathways are some of the most differentially expressed genes between late and early NMPs, showing a peak of expression mid-axial elongation, when NMP numbers peak and lead to maximal production of both presomitic mesoderm and somites. Wnt signalling is essential to drive this increase in NMP numbers during E8.5–E9.5 (Wymeersch et al., 2016). Together with the observation that cells lacking the Wnt response gene *Cdx2* (a crucial axis elongation factor) can be rescued by transplantation to a wild-type environment (Bialecka et al., 2010), this indicates that NM bipotency is not intrinsically determined, but rather relies on the appropriate combination of extrinsic cues that may include modulation of at least Wnt, but possibly also Fgf and Notch signalling levels. This is in line with evidence that the Wnt-expressing milieu is sufficient to maintain axial progenitors lacking zebrafish *ntl* (the zebrafish equivalent of *T*), another crucial Wnt response gene required for axis elongation (Martin and Kimelman, 2010). Intriguingly, the transcriptome of the adjacent notochord progenitors remains relatively stable throughout embryonic axis elongation (Wymeersch et al., 2019). Removal of these cells indicates a crucial role in trunk elongation (Ang and Rossant, 1994; Wymeersch et al., 2019) and suggest that they may also be central to NMP maintenance.

NMP differentiation appears to be driven by signal-induced potentiation of cross-repressive, lineage-specific gene regulatory network activities, which co-exist in bipotent cells (**Table 1, 2; Fig. 5**). *In vivo* and *in vitro* data show that the transition of NMPs into paraxial mesoderm is mediated by elevated canonical Wnt/β-catenin and Fgf signalling levels, which trigger *T* upregulation, downregulation of the pro-neural transcription factor *Sox2*, and the induction of downstream pro-mesodermal transcription factors, such as *Tbx6* and *Msgn1*, which are associated with the somitogenesis clock together with activation of Notch signalling components (Chalamalasetty et al., 2011; Chalamalasetty et al., 2014; Garriock et al., 2015; Gouti et al., 2017; Hofmann et al., 2004; Javali et al., 2017; Koch et al., 2017; Takemoto et al., 2011; Yasuhiko et al., 2006) (**Fig. 5B**). Interestingly, this process involves the induction of an intermediate *Sox2⁺Tbx6⁺* NMP-like cell population resident in the anterior PS and tail bud (Javali et al., 2017). This entity may correspond to the recently described mesoderm-fated NMPs shown to undergo an incomplete EMT (termed 'tbEMT') during the formation of the tail bud (Dias et al., 2020) (**Fig. 5B**). BMP signalling also appears to play a role in the maintenance of early paraxial mesoderm progenitors at tail bud stages (Sharma et al., 2017), in addition to its function as an inducer of LPMP and intermediate mesoderm fates (Edri et al., 2019a; Row et al., 2018; Wymeersch et al., 2019).

The generation of neural derivatives of NMPs requires downregulation of pro-mesodermal transcription factors and signals (e.g. Wnt/Fgf/*T*/*Tbx6*) by retinoic acid (RA) from somites (Diez del Corral et al., 2002; Gouti et al., 2017; Martin and Kimelman, 2010; Martin and Kimelman, 2012; Molotkova et al., 2005; Olivera-Martinez et al., 2012). This involves the initial production of posterior neural progenitors from NMPs, marked by the upregulation of *Sox2* and concomitant restriction of *T/Tbx6* activities, likely due to lower levels of/shorter exposure to Wnt and Fgf signalling, which control *Sox2* expression in the caudal epiblast through activation of the N-1 enhancer (Delfino-Machin et al., 2005; Diez del Corral et al., 2002; Diez del Corral et al., 2003; Javali et al., 2017; Koch et al., 2017; Takemoto et al., 2011). Moreover, Wnt and Notch signals have been shown to further regulate early posterior neural progenitor maintenance and differentiation (Akai et al., 2005; Olivera-Martinez and Storey, 2007; Takemoto et al., 2006) (**Fig. 5B**).

NMP dynamics and the vertebrate body plan

The production of axial tissues is a highly coordinated process that involves the generation of NMP descendants in nascent mesoderm or neurectoderm and their eventual allocation and patterning at a specific location along the A-P axis (**Fig. 6**). The terminal positional identity/patterning of NMP derivatives is determined by the timing of their emergence within the posterior progenitor niches and is largely down to the actions of Hox family members, which are arranged as paralogous groups (PG1–13) in four chromosomal clusters (A,B,C and D). In vertebrates, Hox gene expression is initiated in the posterior of the embryo, in a temporally progressive (collinear) fashion that reflects their 3′-5′ genomic order (i.e. members of PG1 are activated first and PG13 last) [(Denans et al., 2015; Wacker et al., 2004); reviewed in (Deschamps and van Nes, 2005; Mallo et al., 2010)]. As mentioned above, the 'resetting' of chick tail bud NMPs to an 'earlier' state following their engraftment to the NSB of younger hosts, is accompanied by the reprogramming from a Hox PG10⁺ to a Hox PG8⁺ identity (McGrew et al., 2008). This suggests that the Hox code in axial progenitors is labile and sensitive to environmental cues. Based on molecular, genetic and genome-wide analyses, we outline below the potential dynamic interplay between Hox PG member activity and key axial progenitor transcription factors/signals driving morphogenesis during axial elongation. In the mouse embryo, where targeted mutations have elucidated some of the genetic circuitry of axis elongation, the process can be divided into three major phases, with two intervening, 'transitional' phases (**Fig. 7**).

Early phase (<E7.0, <neural plate stage):

Wnt and Fgf signalling delimit the posterior region, triggering the induction of *T* and *Cdx2* and activating early Hox genes belonging to PG1-4 in a Cdx-independent manner (Amin et al., 2016; Neijts et al., 2017). RA is present (Ribes et al., 2009) and can induce early Hox expression, also stimulating expression of the RA-catabolising enzyme *Cyp26a1* (Cunningham et al., 2016).

Transitional early-mid phase (E7.5, head fold stage)

Cyp26a1 expression becomes established, RA is cleared from the PS (Ribes et al., 2009) and the principal regulator of embryonic pluripotency *Oct4* begins to be downregulated (Osorno et al., 2012). PG5-9 Hox genes are activated mainly by Wnt/Fgf, rather than RA, via the action of Cdx2/4 (Amin et al., 2016; Gouti et al., 2014; Hackland et al., 2019; Lippmann et al., 2015; Mazzoni et al., 2013; Metzis et al., 2018; Young et al., 2009) and will take at least 24h to reach maximal expression levels (Gouti et al., 2017; Wymeersch et al., 2019). Wnt/Fgf activities, acting via *T*/*Cdx2* and the simultaneous lowering of RA signalling, lead to the induction of NMPs (Amin et al., 2016; Garriock et al., 2015; Gouti et al., 2017; Gouti et al., 2014; Turner et al., 2014; Wymeersch et al., 2016). At this stage, the pluripotency factors *Oct4* and *Sall4* are re-purposed to act in maintenance and/or differentiation of axial progenitors (Aires et al., 2016; Tahara et al., 2019). *Oct4* in particular, plays a subsequent role in stimulating trunk growth by delaying the activation of posterior Hox PG10-13 members, which are associated with the trunk-to-tail transition (Aires et al., 2016) (see below).

Mid phase (E8.5; 2–5 somites)

This stage coincides with an increase in the numbers of axial progenitors/NMPs under the influence of Fgf and Wnt3a/β-catenin signalling (Garriock et al., 2015; Wymeersch et al., 2016), which are also responsible for a maximal increase in PG4-9 gene expression. Interestingly, expression of PG4-9 members *Hoxa5* and *Hoxb8* (in combination with Wnt signalling) stimulate trunk elongation (Young et al., 2009), suggesting that trunk growth is linked to the increase in PG4-9 expression between the 5–10-somite stage. Expression of *Gdf11*, a BMP/TGFβ family member that is crucial for the relocation of axial progenitors from the NSB/CLE/PS regions to the tail bud (Jurberg et al., 2013), is upregulated in the CLE (Nakashima et al., 1999) and downregulates *Oct4* while further upregulating *Cyp26a1* (Aires et al., 2016; Jurberg et al., 2013). RA activity is almost absent from the posterior end (Sirbu and Duester, 2006). Hox PG10-12 genes, whose expression begins at this stage, are also Wnt/Fgf responsive, require the absence of RA and *Oct4*, and are stimulated by Gdf11 (Aires et al., 2016; Lippmann et al., 2015; Mazzoni et al., 2013). Moreover, Wnt3a induces *Wnt5a* via Cdx binding (Amin et al., 2016; Takada et al., 1994).

Transitional mid-late phase (E9.5, 22–25 somites)

The stage at which *Oct4* is absent (Osorno et al., 2012) and RA activity is undetectable (Cunningham et al., 2011; Sakai et al., 2001) potentially facilitating maximal expression of PG10-12 genes. NMP numbers peak at this stage (Wymeersch et al., 2016). Hox PG13 genes are induced at this point, possibly driven by *Gdf11* (Aires et al., 2019) and Fgf signalling activity (Hackland et al., 2019). Canonical Wnt/β-catenin activity decreases whilst *Wnt5a* remains high and promotes tail outgrowth (in collaboration with *Wnt11*), gradually releasing NMPs from the progenitor region EMT (Andre et al., 2015).

Late phase (>E10.5, >30 somites)

This phase is marked by an increase in the expression of Hox PG13 members, which bind to Cdx2 target sequences, reduce Wnt-driven *T* expression and consequently NMP numbers (Amin et al., 2016; Denans et al., 2015), leading to the eventual exhaustion of progenitors for axial elongation. Genes upregulated at E13.5 (Wymeersch et al., 2019) may affect the final extinction of axial progenitors, as well as tail bud remodelling to remove the neural tube, notochord and tail bud mesoderm.

Species-specific variation

In other vertebrates, including those with highly divergent somite numbers such as snakes, the size of the presomitic mesoderm and somites has been shown to peak midway through axis elongation (Gomez et al., 2008). This argues that, as in mouse, a stepwise mechanism dependent on multiple temporal feedbacks is likely to operate in animals with diverse body plans. For example, the onset of *Gdf11* expression has been correlated with the position of the hindlimb primordia in various species (Matsubara et al., 2017) and extended Oct4 activity in snake, with a long trunk and relatively short neck and tail, may support trunk expansion (Aires et al., 2016).

Axial progenitors *in vitro*

Capturing NM-potent cells in vitro

The limited numbers of microdissected embryonic axial progenitors is a major obstacle to the study of their genetic and epigenetic regulation, for example through biochemical approaches requiring large amounts of starting material. Moreover, obvious ethical and practical reasons preclude the study of axial progenitors in human embryos. The *in vitro* generation of large numbers of axial progenitors from PSCs offers an attractive alternative approach addressing these issues. Furthermore, *in vitro*-derived axial progenitors can act as a promising source of posterior spinal cord and mesodermal cell types, specifically at thoracic and lumbosacral levels, which could be employed for disease modelling and cell replacement applications. Early hallmarks of *in vitro*-derived NMP-like cells, such as emergence of T^+Sox2^+ cells and upregulation of transcripts marking NMP-containing regions (e.g. *Cdx2*, *Fgf8* and Hox genes), were first reported in mouse epiblast stem cell (mEpiSCs) cultures treated with the Wnt agonist/Glycogen synthase kinase 3 (GSK3)-inhibitor CHIR99021 (CHIR) in combination with FGF2 and Activin A (Tsakiridis et al., 2014). This subpopulation comprised a distinct, minor entity within cultures dominated by T^+Foxa2^+ mesendodermal progenitors. Interestingly, when cells from these cultures were grafted into the NSB of E8.5 mouse embryos, they colonised both the neural tube and paraxial mesoderm, indicating their bipotency (Tsakiridis et al., 2014).

A number of reports have been subsequently published, describing improved protocols for the directed differentiation of both human (hPSCs) and mouse PSCs (e.g. mouse embryonic stem cells; mESCs and mEpiSCs) into T^+Sox2^+ cultures (Amin et al., 2016; Cooper, 2020; Cunningham et al., 2016; de Lemos, 2019; Denham et al., 2015; Diaz-Cuadros et al., 2020; Edri et al., 2019a; Edri et al., 2019b; Frith et al., 2018; Gouti et al., 2014; Hackland et al., 2019; Kirino et al., 2018; Kumamaru et al., 2018; Lippmann et al., 2015; Row et al., 2018; Tsakiridis and Wilson, 2015; Turner et al., 2014; Verrier et al., 2018) (**Table 3**). Despite variations in terms of treatment duration, media composition and choice of signalling agonists/coating substrates, all protocols for the *in vitro* generation of axial progenitors rely on the stimulation of the Wnt and, often, Fgf signalling pathways (**Fig. 8**), thus recapitulating the signalling environment of progenitor niches *in vivo* (**Table 2; Fig. 5**). Resulting PSC-derived cell populations expressed caudal markers (Edri et al., 2019b; Frith et al., 2018; Gouti et al., 2017; Gouti et al., 2014; Verrier et al., 2018), exhibited the ability to generate neural and mesodermal cell types *in vitro* (Frith et al., 2018; Gouti et al., 2014; Turner et al., 2014) and/or contributed to both the neural tube and paraxial mesoderm after engraftment into host chick or mouse embryos (Baillie-Johnson et al., 2018; Edri et al., 2019a; Gouti et al., 2014) (**Table 3**). Embryo grafting in these cases has provided a useful assay for the developmental potential of *in vitro*-derived axial progenitors although the early somite mouse embryo appears to offer a more stringent host environment for distinguishing between NM bipotency vs pluripotency compared to their late gastrula chick counterparts (Baillie-Johnson et al., 2018; Gouti et al., 2014; Huang et al., 2012; Tsakiridis et al., 2014).

NMP-like cells have also been reported to arise in a regionalised manner, in three-dimensional (3D), self-organising aggregates of PSCs following a short timed pulse of CHIR (Beccari et al., 2018; Faustino Martins et al., 2020; Libby, 2020; Turner et al., 2014; van den

Brink et al., 2020; Veenvliet, 2020). These organoid-like structures show signs of A-P and dorsoventral axis formation, polarised collinear Hox gene activation and somitogenesis (Beccari et al., 2018; van den Brink et al., 2020; Veenvliet, 2020), and thus comprise an attractive model to study early morphogenetic axis elongation events. These data collectively suggest NMP-like cells can be generated *in vitro* from PSCs and these can act as a source of differentiated axial tissue derivatives that resemble their *in vivo* counterparts. However, the various *in vitro*-derived NMP-like populations that have been reported appear to be quite different both at a transcriptome level and in terms of their differentiation potential. This is likely due to the use of differing culture regimes and starting PSC populations (mESCs, mEpiSCs, hPSCs) resulting in the generation of progenitor populations corresponding to a continuum of developmental states, ranging from the late gastrula caudal epiblast up to tail bud stages (Edri et al., 2019a; Edri et al., 2019b; Frith et al., 2018; Gouti et al., 2017; Gouti et al., 2014; Verrier et al., 2018). Furthermore, the culture conditions that induce T^+Sox2^+ cells from PSCs also appear to promote the emergence of LPMPs and intermediate mesoderm progenitors, as revealed by the expression of associated markers (Edri et al., 2019a; Row et al., 2018), indicating the induction of heterogeneous cultures that contain a mixture of posterior axial progenitor subpopulations.

It should be noted that, thus far, none of these protocols have demonstrated the existence of truly bipotent cells, as defined by the ability of a single cell to generate both neural and mesodermal derivatives. Previously, we attempted to interrogate the potency of single cells via the clonal plating of FACS-sorted T-GFP reporter-positive mEpiSC-derived NMP-like cells in the presence of Wnt and Fgf agonists. Through this approach we showed mixed neural and mesodermal colonies could be generated from single T-GFP$^+$ cells, although the majority of the resulting colonies consisted exclusively of Sox2$^+$ neural cells, suggesting either a neural bias of NMPs or neural-favouring plating/culture conditions (Tsakiridis and Wilson, 2015). Moreover, *in vitro*-derived NMP-like cells are a transient entity both *in vivo* and *in vitro*, and attempts to maintain homogeneous cultures of T^+Sox2^+ cells over extensive time periods (>3 passages) in the presence of Wnt and Fgf agonists (i.e. the conditions promoting their induction) have thus far been unsuccessful. In all cases, cultures tend to gradually downregulate *T* and other NMP-specific markers and differentiate into their downstream derivatives (Cooper, 2020; Edri et al., 2019a; Gouti et al., 2017; Tsakiridis and Wilson, 2015; Wind, 2020).

Interestingly, single-cell RNA sequencing data have revealed a subpopulation of cells expressing node-associated transcripts (*T, Foxa2, Noggin, Chordin, Shh*) that co-emerges with NMP-like cells during their induction from mEpiSCs (Edri et al., 2019b). Some of these markers have also been detected in hPSC-derived NMP-like cultures (Denham et al., 2015; Frith et al., 2018). It is tempting to speculate, based on evidence from co-culture experiments

(Edri et al., 2019b), that these node-like cells facilitate the maintenance of an T^+Sox2^+ NMP identity *in vitro* and their progressive elimination upon prolonged culture may be responsible for the exhaustion of NMP-like cells. Additional experiments are required to properly dissect cell-autonomous versus non-autonomous aspects of NMP self-renewal *in vitro*.

In vitro-derived axial progenitors as a source of 'hard-to-make' posterior cell types

The A-P axial identity of PSC derivatives is likely to shape their functionality and developmental/regenerative potential as demonstrated by xenotransplantation experiments in animal models (Kadoya et al., 2016; Peljto et al., 2010). As various congenital birth defects and neurodegenerative conditions affect certain cell types in an axial level-specific manner (**Box 2**), their *in vitro* modelling relies not only on generating from PSCs cell populations of the correct lineage, but also the appropriate axial identity (Allodi et al., 2019; An et al., 2019; Gordon et al., 2014; Vega-Lopez et al., 2018).

Posterior spinal cord

Until recently, the directed differentiation of PSCs towards neural derivatives has been heavily influenced by Nieuwkoop's 'activation-transformation' model and the idea that anterior neurectoderm is induced 'by default' in the absence of posteriorising signals, which can be further patterned by RA/Wnt signals to induce progressively more posterior neural cells (Chambers et al., 2009; Nieuwkoop and Nigtevecht, 1954). However, this approach predominantly gives rise to hindbrain or anterior (cervical/brachial) spinal cord derivatives and fails to efficiently generate cells of a more caudal identity (e.g. thoracic/lumbosacral) *in vitro* (Imaizumi et al., 2015; Kirkeby et al., 2012; Maury et al., 2015; Meinhardt et al., 2014). The *in vitro* derivation of NMP-like cells paved the way for a new generation of differentiation protocols that instead rely on the production of a Wnt-Fgf-induced T^+Sox2^+ NMP/posterior pre-neural intermediate state from PSCs, and its subsequent 'neuralisation' via addition of RA and inhibition of TGF/Nodal and/or BMP signalling pathways (**Fig. 8**). This strategy has led to the production of neurectodermal cells corresponding to the thoracic and lumbosacral regions (Cooper, 2020; Frith et al., 2018; Gouti et al., 2014; Kumamaru et al., 2018; Lippmann et al., 2015; Mouilleau, 2020; Verrier et al., 2018; Wind, 2020). Interestingly, these cells can be passaged and expanded as spinal cord neural stem cells over extended time periods (Cooper, 2020; Kumamaru et al., 2018) and further directed to produce neurons of distinct dorsoventral identities (Cooper, 2020; Kumamaru et al., 2018; Lippmann et al., 2015; Verrier et al., 2018; Wind, 2020). More recent reports have combined micropatterning and 3D organoid-based approaches with the induction of NMP-like cells in order to increase reproducibility, dissect signalling dynamics in spinal cord cells, or study interactions between NMP derivatives such as skeletal muscle and spinal cord neurons in neuromuscular organoids (Duval et al., 2019;

Faustino Martins et al., 2020; Knight et al., 2018; Mouilleau, 2020). Evidence from transplantation experiments in a rat spinal cord injury model has suggested that posterior spinal cord cells derived from PSCs via a NMP intermediate may offer a promising avenue toward the development of cell replacement therapies (Kumamaru et al., 2018), yet further characterisation of these cells is required to better define their value in a clinical context.

Wnt/Fgf-triggered induction of NMP-like cells is accompanied by sequential upregulation of Hox family members up to PG9 thus reflecting a predominantly posterior brachial and thoracic character (Lippmann et al., 2015) (**Fig. 6**). A shift to more posterior Hox PGs, corresponding to lumbosacral levels, can only be achieved through increased Fgf signalling activity and/or treatment with GDF11, a key regulator of trunk-to-tail transition during embryonic axis elongation, as well as caudal Hox expression (Aires et al., 2019; Hackland et al., 2019; Jurberg et al., 2013; Lippmann et al., 2015; Liu et al., 2001; Mouilleau, 2020). However, despite the reported production of lumbar motor neurons through this approach (Lippmann et al., 2015; Mouilleau, 2020), there is still limited quantitative/functional evidence regarding its efficiency and more research is needed to understand the optimal conditions for generating tissues of defined sections of the postcranial axis.

PSC-derived T^+Sox2^+ cells are also an efficient source of posterior neural crest (NC), the multipotent embryonic cell population that arises in the dorsal neural plate/non-neural ectoderm border region and acts as a source of various cell types including peripheral neurons. Similar to central nervous system derivatives, the conventional route to obtain NC cells *in vitro* has relied on the production of an anterior neurectodermal intermediate that is subsequently steered towards NC fate through stimulation of Wnt/BMP signalling (to recapitulate the neural plate border environment). However, this method has been inefficient in producing trunk or lumbar NC (Hackland et al., 2017; Lee et al., 2007; Menendez et al., 2011). Wnt/FGF-treated hPSC cultures contain a T^+ subpopulation that exhibit features of early NC precursors arising at the border of the caudal neural plate *in vivo*. These findings have led to the establishment of differentiation protocols for the efficient generation of trunk NC cells and their sympathoadrenal derivatives *in vitro* (Abu-Bonsrah et al., 2018; Cooper, 2020; Denham et al., 2015; Frith et al., 2018; Frith and Tsakiridis, 2019; Gomez, 2019; Hackland et al., 2019). The resulting trunk NC cells are derived from T^+ cells within hPSC-derived NMP-like cultures (Frith et al., 2018). Moving forward, single-cell lineage tracing experiments are required to map more precisely the segregation dynamics of posterior NC, spinal cord neurectoderm and paraxial mesoderm as well as the origin of their progenitors both during PSC differentiation and *in vivo*.

Paraxial mesoderm/skeletal muscle

A number of recent PSC-differentiation protocols have also been shown to efficiently produce paraxial mesoderm and skeletal muscle via the early induction of T^+Sox2^+ NMP-like cells (**Fig. 8**) (Chal et al., 2016; Diaz-Cuadros et al., 2020; Loh et al., 2016; Sudheer et al., 2016; Xi et al., 2017). These studies have provided valuable insights into the molecular and signalling basis of early paraxial mesoderm specification (Diaz-Cuadros et al., 2020; Loh et al., 2016; Sudheer et al., 2016) opening new avenues toward cell replacement and disease modelling applications (Chal et al., 2016). Since axial progenitors closer to the node (e.g. NMPs) give rise preferentially to medial somites, whereas their more caudal PS counterparts tend to exhibit more lateral somite contribution (Cambray and Wilson, 2007), it would be interesting to exploit such PSC-based systems in order to dissect the effect of various signals on the propensity of axial progenitors to generate medial versus lateral somite derivatives.

Lateral plate/intermediate mesoderm

PSC differentiation studies have also indicated that endogenous BMP signalling is crucial in regulating the balance between paraxial mesoderm (requires BMP inhibition) and lateral plate mesoderm/neural crest cell (BMP-dependent) fates within *in vitro*-derived NMP-like cultures (Frith et al., 2018; Loh et al., 2016; Row et al., 2018; Xi et al., 2017). These data are in line with findings from *in vivo* studies showing that the balance between Fgf and BMP signalling (and their downstream bHLH effectors) in mesodermal progenitors is crucial in assigning a mediolateral fate (Miura et al., 2006; Row et al., 2018). Moreover, T^+ axial progenitors, induced from PSCs following Wnt stimulation, appear to be competent to generate intermediate mesoderm and, subsequently, Wolffian duct cells and nephric mesenchyme (Taguchi et al., 2014; Taguchi and Nishinakamura, 2017; Takasato et al., 2015). These data are consistent with lineage-tracing experiments in mouse embryos showing that E7.5 and E8.5 T^+ axial progenitors give rise to the Wolffian duct and meso/metanephric mesenchyme, respectively (Taguchi et al., 2014), as well as embryo grafting studies where only contribution to the nephrogenic mesenchyme was observed from the CLE (Cambray and Wilson, 2007; Wymeersch et al., 2016).

Conclusion and future perspectives

Embryonic axis elongation has been in the research spotlight for a long time, being a valuable paradigm of a crucial, evolutionarily-conserved developmental process. The discovery that it is driven by stem cell-like progenitors with the ability to generate both neural and mesodermal derivatives has challenged conventional views about the nature of cell lineage, germ layers and multipotency. The combination of classic embryology techniques with recently established 2D and 3D PSC-based *in vitro* systems and cutting-edge imaging/single cell sequencing approaches has provided unprecedented insights into the cellular and molecular basis of axial progenitor fate decisions and behaviour. These will continue to be powerful tools in future efforts to increase our understanding of axis elongation and associated birth defects, especially when used in conjunction with genetic perturbation experiments, controlled artificial microenvironments (e.g. through the use of micropatterning/microfluidics platforms), and may include input from other disciplines such as mathematics, physics and engineering. The next obvious research direction will involve the implementation of spatial transcriptomics and quantitative hybridization chain reaction methods (Choi et al., 2018; Eng et al., 2019; Junker et al., 2014; Rodriques et al., 2019) to record gene expression profiles of single embryonic axial progenitor cells *in situ.* Such studies are crucial for the definitive spatiotemporal mapping of the interplay between niche signals, downstream transcriptional read-outs and cell behaviour (fate/ potency) within the native context of the embryo. Moreover, these could be expanded to include also the analysis of chromatin landscape/higher order chromosomal organisation changes associated with distinct phases of axis elongation. To further address key questions on how tissue scaling, de-coding of positional information and homeostasis of axial progenitor pools are coordinated during the construction of the body plan, the comparative study of a wide range of diverse and novel animal models is essential, extending earlier findings from previous cross-species studies (Aires et al., 2016; Gomez et al., 2008; Steventon et al., 2016). Finally, additional work building on key findings from pioneering studies that indicate the role of tissue mechanics (Mongera et al., 2018), signalling-gene expression dynamics (Lauschke et al., 2013; Matsuda et al., 2020; Sonnen et al., 2018) and metabolism (Bulusu et al., 2017; Oginuma et al., 2017) in embryonic axis elongation is required.

Acknowledgements

We would like to thank Kate G. Storey and David Kimelman for sharing immunostaining images and Anahi Binagui-Casas for critical reading of the manuscript. We apologise to colleagues whose work could not be cited owing to space constraints.

Competing interests

None

Funding

The authors' research is supported by BBSRC (New Investigator Research Grant, BB/P000444/1; AT), H2020-EU.1.2.2 (Grant agreement ID: 824070; AT), Children's Cancer and Leukaemia Group/Neuroblastoma UK (CCLGA 2019 28; AT), MRC (MR/S008799/1; VW and MR/V002163/1; AT) and a JSPS KAKENHI grant (JP19K16157; F.J.W).

Box 1. Glossary.

Amnion: An extraembryonic membrane enveloping the embryo in amniote species thus providing protection.

Axial progenitors: A collective term to describe the progenitor cells located in the caudal progenitor zone, which together drive axial elongation. Axial progenitors arise at the end of gastrulation, give rise to the posterior tissues from the neck down, and show differences in **fate** and **potential (potency)**.

Chordoneural hinge (CNH): A term originating from frog studies (Gont et al., 1993). The CNH is the location in the tail bud on the ventral midline where the neural tube (floorplate) and the underlying notochord are continuous. In frog, it is derived from the dorsal blastopore lip; in mouse and chick it is principally derived from the node-streak border (NSB).

Fate/potency: Cell '**fate**' describes the normal descendants of a cell in an undisturbed embryo. Potency denotes cells' capacity to adopt additional identities if challenged with a different (heterotopic) environment. Thus, some NMPs with neuromesodermal **potency** (defined by heterotopic grafting) do not adopt both fates, although a subset of NMPs are dual-fated (defined by **fate mapping** and clonal analysis).

Fate mapping: The process of prospectively charting the final location and identity of single or groups of cells in defined embryonic regions. This involves following the progeny of labelled cells (carrying e.g. a genetic marker such as GFP or topically marked with fluorescent dyes) at a known location through a period of developmental time.

Gastrulation: A phase of early embryonic development during which a single cell layer epithelium forms three germ layers: ectoderm, mesoderm and endoderm, which serve as the building blocks of all cell types in the embryonic body. This process involves a sequence of coordinated morphogenetic movements that direct the ingression of cells through a structure called the **primitive streak (PS)** in amniotes, the **blastopore** in amphibians and the **germ ring** in fish.

Intermediate mesoderm: Mesodermal subtype positioned between the paraxial and lateral plate mesoderm, which gives rise to the urogenital system (including the kidney and gonads).

Lateral plate mesoderm (LPM)/ventral mesoderm: Mesodermal subtype that is further split into dorsal (splanchnopleure) and ventral (somatopleure) layers, which underlie the ectoderm and overlie the endoderm, respectively. The LPM/ventral mesoderm gives rise to structures such as the heart, body wall, blood vessels and blood cells and lymphatic vessels.

Myotome: muscle precursors derived from paraxial mesoderm**.**

Neurenteric canal: In the frog, the neurenteric canal is connection formed between the lumen of the spinal cord and that of the gut. In human, it connects the amniotic cavity and the yolk sac during early embryo development. It is likely an ancestral chordate feature and present in some (e.g. Amphioxus, shark, frog, turtle, gecko, human), but not all organisms (e.g. mouse or chick).

Notochord: A rod-like mesodermal structure that stretches along the entire anteroposterior axial midline and plays a crucial role in patterning processes such as dorsal-ventral regionalisation of the neural tube.

Organiser (Node, dorsal blastopore lip, shield): Structure that contains notochord progenitors and is conserved amongst vertebrate embryos (termed **node** in amniotes, **dorsal blastopore lip** in amphibians and **shield** in fish) with the ability, early during gastrulation, to organise a secondary neural axis when transplanted to an ectopic site.

Paraxial mesoderm: Mesoderm that lies on either side of the midline. This includes the somites and unsegmented presomitic mesoderm.

Presomitic mesoderm: Paraxial mesoderm that generates the somites via a segmentation process. The somites lie on either side of the neural tube and act as the precursors of the musculoskeleton.

Retrospective clonal analysis: Analysis of the clonal progeny of a cell that has been heritably labelled at random to define cell behaviour and lineage segregation at distinct time-points. One such strategy relies on the spontaneous reversion of a 'laacZ gene', carrying an inactivating sequence duplication, to an active lacZ reporter via rare intragenic homologous recombination within the duplication.

Trunk-to-tail transition: Developmental period in which the caudal progenitor zone changes from laying down trunk tissues to forming a tail bud, after which tail growth can commence.

Box 2. Birth defects and axial progenitors

Some birth defects affecting axial structures arise due to mutations in regulators of axial progenitor maintenance/differentiation. Retinoic acid (RA) and its mimetics can cause axial truncations in both mouse and human, similar to caudal regression syndrome (Padmanabhan, 1998). Studies in mice suggest that RA is potentiated by high levels of foetal glucose, linking it to maternal diabetes (Chan et al., 2002). RA attenuates Wnt signalling (Shum et al., 1999) and its direct target *T*. Interestingly, a large mass of tissue at the level of the hindlimb bud arises when either *T* is mutated or excess RA is present during development (Padmanabhan, 1998; Schmidt et al., 1997). Exposure of E9.5 mouse embryos to etretinate (an RA mimetic) similarly leads to persistence of a caudal mass of neural-like tissue (Liu et al., 2003), suggesting a secondary effect of retinoids in maintaining this tissue. This phenotype resembles Currarino and VACTERL syndromes in humans, which have been associated with aberrant expression of axial progenitor-related genes such as *MNX1*, *GDF11* and *HOX* family members (Szumska et al., 2008; Wymeersch et al., 2019). Moreover, segregation/linkage analyses in families and patient sequencing data have revealed that mutations in *T* are directly linked to cases of neural tube defects (NTDs), sacral agenesis and congenital vertebral abnormalities (Agopian et al., 2013; Carter et al., 2011; Fellous et al., 1982; Ghebranious et al., 2008; Jensen et al., 2004; Morrison et al., 1996; Postma et al., 2014; Shields et al., 2000). The links between NTDs and defects in axial progenitor differentiation/impaired morphogenesis are further reinforced by the demonstration that axial progenitor-containing regions during mouse development participate in neural tube closure (Anderson et al., 2016; Dady et al., 2014; Galea et al., 2017; Lopez-Escobar et al., 2018; Zhao et al., 2014). Collectively, these findings suggest that understanding anteroposterior axis development can provide valuable insights into the genetic and environmental factors that lead to abnormalities of caudal development and *vice versa*.

Box 3. NMPs are epithelial

Several lines of evidence support the idea bi-fated NMPs are epithelial throughout axis elongation. Lineage labelling of the epiblast early during axial elongation (Cambray and Wilson, 2007; Wilson and Beddington, 1996; Wymeersch et al., 2016) or the posterior neural tube in the tail (Cambray and Wilson, 2002; Wilson and Beddington, 1996), produces descendants in both neural tube and mesoderm. Retrospective clonal analysis has shown that clones generally contribute unilaterally in the neurectoderm and bilaterally in the mesoderm, suggesting a net movement from the caudal lateral epiblast to the mesoderm via EMT. Moreover, in most NM clones the anterior limit in neurectoderm is more anterior than that in mesoderm (Tzouanacou et al., 2009). Several of these clones show additional contribution to neural crest at their anterior-most end, which suggests that they are initiated in the lateral neural plate and their descendants moved towards the midline, eventually forming mesoderm. The potential of the posterior end of the prospective neurectoderm in the tail bud to form mesoderm has been demonstrated in vertebrates as diverse as chick (Olivera-Martinez et al., 2012) and axolotl (Taniguchi et al., 2017). Thus, the identity of NMPs is most likely epithelial (the dorsal NSB, CLE and dorsal CNH) throughout axis elongation.

Figure legends

Fig. 1. Axial progenitors give rise to the vertebrate axis. (A) Diagrams of an E8.75 mouse embryo (~9–12 somites; Theiler Stage (TS) 13) with boxes showing the posterior (Aa) and anterior (Ab) axis. (Aa) Posteriorly, epiblast progenitors (cyan) that move towards the primitive streak can undergo EMT (grey arrows). As daughter cells move away from the streak and rostrally, they form the presomitic mesoderm (pink). Epiblast progenitors at more caudal locations (not depicted) give rise to intermediate and lateral mesoderm (white arrows). Epiblast progenitors that persist in the epithelium form the neural tube (black arrows). (Ab) Anteriorly, the neural epithelium closes to form the future spinal cord, with neural crest (dark green) forming dorsally and floor plate ventrally (green). Mesoderm subtypes include somites (paraxial mesoderm; pink), intermediate (IM; lavender) and lateral/ventral mesoderm (LVM; pale pink). (B) Neuromesodermal progenitors (NMP, cyan), lateral and paraxial mesoderm progenitors (LPMP, gold), notochord progenitors (NotoP, red) and the axial tissues they give rise to (solid lines) or have the potency to form (dashed lines). A, anterior; D, dorsal; P, posterior; V, ventral.

Fig. 2. Axial progenitor locations in mouse. (A) Wholemount images and schematics illustrating the mouse caudal progenitor zone. (Aa-Ab) At E8.5 (2-5 somites (s); TS12), the primitive streak (PS) area harbours axial progenitors: NMPs (cyan) and LPMPs (gold). (Ac) Ventral view showing the PS from the node anteriorly to the hindgut posteriorly. Lateral from the PS, presomitic mesoderm is formed under the caudal lateral epiblast (CLE). (Ad) Schematic of the dorsal posterior embryo showing the location of axial progenitors in the CLE: anteriorly, the U-shaped area harbours NMPs, whereas LPMPs at the posterior CLE are fated for lateral and ventral mesenchyme. (Ba) DAPI-stained sections with colours illustrating the location of NMPs, LPMPs and NotoPs (red). (Bb) Transverse section through the mid PS. (Bc) magnification of the node region in Ba (box). (Ca) Tail bud-stage embryo (E10.5; 32-35s; TS16) showing the location of the CNH. (Cb) DAPI-stained section showing the location of NMPs. (D) Schematic as in Ad, illustrating NM potency extends further caudally and laterally compared to NM fate at E8.5. cr, crown of the node; dn, dorsal node layer; HF, headfolds; NC,

notochord; NSB, node-streak border; NT, neural tube; PSM, presomitic mesoderm; TBM, tail bud mesoderm; vn, ventral node layer. A, anterior; D, dorsal; L, left; P, posterior; R, right; V, ventral. Asterisk, the crown region also contains progenitors fated for dorsal gut.

Fig. 3. Location of key tissues and axial progenitor cell populations in vertebrates. Schematics showing the location of the caudal progenitor zone in different organisms (red dashed lines; e.g. the CLE/NSB or CNH) and, if known, the location of NMPs or T^+Sox2^+ progenitors (blue). (A-B) In chick, NMP locations are similar to those in mouse: the node-streak border (NSB) the anterior fraction of the caudal lateral epiblast (Ant. CLE) at Hamburger Hamilton stage 8 (HH8), and the chordoneural hinge (CNH) at HH18. At this time, the CLE also harbours axial progenitors other than NMPs (Post. CLE). (C) Left, posterior dorsal view at Stage (St)13 in *Xenopus* shows the dorsal and ventral blastopore lip (dBPL, vBPL) and a sagittal section showing the CNH. (D) Lateral view and sagittal section of a St28 embryo. (E-F) Lateral views on zebrafish embryos at 6 somite (s) and 26s stage, showing the stem zone. At tail bud stages, ntl^+sox2^+ cells have been shown to reside in the stem zone. (G) Dorsal view on a Carnegie stage (CS) 9 (~3s) human embryo with the box showing a sagittal section through the PS and neurenteric canal. (H) Lateral view of a CS12 (25s) embryo; T^+Sox2^+ cells have been shown to reside in the tail bud. Diagrams based on (Beck and Slack, 1998; Kimmel et al., 1995; Muller and O'Rahilly, 2004; Rulle et al., 2018; West, 1937; Wilson et al., 2009) and www.xenbase.org. NC, notochord; NT, neural tube; PS, primitive streak; PSM, presomitic mesoderm; TB, tail bud; TBM, tail bud mesoderm. A, anterior; P, posterior.

Fig. 4. NMP location coincides with T^+Sox2^+ expression in vertebrate embryos. In the vertebrate embryonic tail bud, NMPs are located within the T/SOX2 double-positive expression domain (encircled by white dashed lines): mouse (A), chick (B), zebrafish (C) and human embryos (D). Ntl is the zebrafish homologue of T. Asterisk, notochord end. Images adapted from (Martin and Kimelman, 2012; Olivera-Martinez et al., 2012; Wymeersch et al., 2016).

Fig. 5. Gene expression in the mouse caudal progenitor zone. (**A**) Schematic of the dorsal posterior embryo illustrating Sox2 (green) and T (magenta) expression in relation to neural (N) vs mesodermal (M) fate choices of NMPs (cyan dashed line) and LPMPs (gold dashed line). Cell differentiation trajectories are represented by directional black (N) or white arrows (M) respectively, with their length indicating proportions of cells entering each lineage, e.g. T^+Sox2^+ NMPs in the anterior CLE have equal capacity to form N or M tissues, whereas those closer to the posterior or midline are likely to contribute to the mesoderm. NotoPs (red dashed

line) are located ventrally and express high levels of *T*. The expression profile for different axial progenitors is based on expression data from (Wymeersch et al., 2016; Wymeersch et al., 2019). A, anterior; L, left; P, posterior; R, right. (**B**) Model for $T^{+}Sox2^{+}$ NMP maintenance and N or M differentiation *in vivo*. Wnt and Fgf signals and lowering of retinoic acid (RA) signalling levels by Cyp26a1 enable NMP maintenance during trunk extension. Some $Sox2^{+}Tbx6^{+}$ NMP-like cells have been shown to partially undergo EMT (termed 'tbEMT'). Developmental signals associated with further commitment toward neurectoderm or presomitic mesoderm are also shown, see see main text for details. (see main text for details).

Fig. 6. Anteroposterior patterning of the vertebrate axis originates in NMPs. The allocation of patterned tissues relates to Hox acquisition in NMPs and their progressive differentiation from the caudal region. Three stages during mouse axis elongation are shown (shades of blue). (A) The activation of Hox paralogous groups (PG) in NMPs during three phases of axis elongation (also see **Fig.7**): anterior Hox PG (1-3; teal), central Hox PG (4-8; yellow), posterior Hox PG (9-12; pink) and terminal Hox PG (13; purple). At each stage, NMP daughter cells (blue circles) can give rise to mesoderm and exit the NSB or CNH (orange arrows). (B) Left, approximate contribution of these mesodermal descendants (shown in A) to the E12.5 embryonic axis. The axial level is indicated by blue shades [e.g. a NMP daughter cell exiting the NSB at 5s will contribute to axial structures at ~13-19s, based on data from (Cambray and Wilson, 2007; Tam, 1986; Wymeersch et al., 2016)]. Right, the number of available NMPs varies depending on the embryonic day (E; represented by relative circle size). As NMP numbers peak at E9.5 (Wymeersch et al., 2016), they will relatively contribute more cells to the PSM (Gomez et al., 2008) and eventually form larger somites (Tam, 1981) (dark blue circles). (C) Hox genes and the vertebrae they pattern (based on Burke et al., 1995; Kuratani, 2009) in relation to the approximate NMP contribution pattern shown in the embryo above (orange dashed lines). Labels in black show the vertebral formula. CNH, chordoneural hinge; NSB, node-streak border; PS, primitive streak; PSM, presomitic mesoderm; TBM, tail bud mesoderm.

Fig. 7. A dynamic regulatory mechanism in NMPs drives axial patterning. Model of how the mouse vertebral pattern is ultimately shaped by the signalling dynamics sensed by NMPs. (A) The pool of available NMPs during murine axis elongation is represented by circles: it is established after gastrulation, expands until ~E9.5 and contracts thereafter (shades of blue are the same as in **Fig. 6**). (B) The signalling environment acting on NMPs can be separated into five phases (grey shades): (1) Activation of early Hox genes in a Cdx-independent manner. At this time Pou5f1 (Oct4) and retinoic acid (RA) are present in the epiblast (orange

triangle) (2) Cdx and T function activate Hox genes up to paralogous group (PG) 9 and downregulate RA via Cyp26a1. (3) Wnt3a induces *Wnt5a* via Cdx binding. (4) Inputs including β-catenin and Fgf signalling promote a maximal increase in PG4-9 genes via Cdx2/4. PG10-12 genes start to be expressed at this stage. (5) Gdf11/Tgfbr1 signalling further stimulates these Hox genes and downregulates *Pou5f1* while upregulating *Cyp26a1*. (6) PG13 genes are triggered, decreasing Wnt3a/β-catenin activity whereas Wnt5a remains high and promotes tail outgrowth.

Fig. 8. Differentiation of human pluripotent stem cells to NMP-like cells and their axial derivatives. (A) $T^{+}Sox2^{+}$ immunostaining showing NMP-like cells, obtained from human ES cells after culture in CHIR 99021 and FGF2 for three days. (B) Diagram showing the key signals/treatments shown to direct pluripotent stem cells (PSC; grey) towards differentiated posterior neural (green) and mesodermal derivatives (pink) via an intermediate NMP-like state (blue), The relevant cell markers are shown in bold. i, inhibitor. Note that the scheme summarises adherent and not 3-dimensional/organoid-based strategies. Non-essential signals/treatments for the induction of the indicated cell types but employed in some studies are shown within brackets.

References

Abu-Bonsrah, K. D., Zhang, D., Bjorksten, A. R., Dottori, M. and Newgreen, D. F. (2018). Generation of Adrenal Chromaffin-like Cells from Human Pluripotent Stem Cells. *Stem Cell Reports* **10**, 134-150.

Agopian, A. J., Bhalla, A. D., Boerwinkle, E., Finnell, R. H., Grove, M. L., Hixson, J. E., Shimmin, L. C., Sewda, A., Stuart, C., Zhong, Y., et al. (2013). Exon sequencing of PAX3 and T (brachyury) in cases with spina bifida. *Birth Defects Res A Clin Mol Teratol* **97**, 597-601.

Aires, R., de Lemos, L., Novoa, A., Jurberg, A. D., Mascrez, B., Duboule, D. and Mallo, M. (2019). Tail Bud Progenitor Activity Relies on a Network Comprising Gdf11, Lin28, and Hox13 Genes. *Dev Cell* **48**, 383-395 e388.

Aires, R., Jurberg, A. D., Leal, F., Novoa, A., Cohn, M. J. and Mallo, M. (2016). Oct4 Is a Key Regulator of Vertebrate Trunk Length Diversity. *Dev Cell* **38**, 262-274.

Akai, J., Halley, P. A. and Storey, K. G. (2005). FGF-dependent Notch signaling maintains the spinal cord stem zone. *Genes Dev* **19**, 2877-2887.

Allodi, I., Nijssen, J., Benitez, J. A., Schweingruber, C., Fuchs, A., Bonvicini, G., Cao, M., Kiehn, O. and Hedlund, E. (2019). Modeling Motor Neuron Resilience in ALS Using Stem Cells. *Stem Cell Reports* **12**, 1329-1341.

Amin, S., Neijts, R., Simmini, S., van Rooijen, C., Tan, S. C., Kester, L., van Oudenaarden, A., Creyghton, M. P. and Deschamps, J. (2016). Cdx and T Brachyury Co-activate Growth Signaling in the Embryonic Axial Progenitor Niche. *Cell Rep* **17**, 3165-3177.

An, D., Fujiki, R., Iannitelli, D. E., Smerdon, J. W., Maity, S., Rose, M. F., Gelber, A., Wanaselja, E. K., Yagudayeva, I., Lee, J. Y., et al. (2019). Stem cell-derived cranial and spinal motor neurons reveal proteostatic differences between ALS resistant and sensitive motor neurons. *Elife* **8**.

Anderson, C. and Stern, C. D. (2016). Organizers in Development. *Curr Top Dev Biol* **117**, 435-454.

Anderson, M. J., Magidson, V., Kageyama, R. & Lewandoski, M. (2020). Fgf4 is critical for maintaining Hes7 levels and Notch oscillations in the somite segmentation clock. *bioRxiv*.

Anderson, M. J., Naiche, L. A., Wilson, C. P., Elder, C., Swing, D. A. and Lewandoski, M. (2013). TCreERT2, a transgenic mouse line for temporal control of Cre-mediated recombination in lineages emerging from the primitive streak or tail bud. *PLoS One* **8**, e62479.

Anderson, M. J., Schimmang, T. and Lewandoski, M. (2016). An FGF3-BMP Signaling Axis Regulates Caudal Neural Tube Closure, Neural Crest Specification and Anterior-Posterior Axis Extension. *PLoS Genet* **12**, e1006018.

Andre, P., Song, H., Kim, W., Kispert, A. and Yang, Y. (2015). Wnt5a and Wnt11 regulate mammalian anterior-posterior axis elongation. *Development* **142**, 1516-1527.

Ang, S. L. and Rossant, J. (1994). HNF-3 beta is essential for node and notochord formation in mouse development. *Cell* **78**, 561-574.

Araki, K., Imaizumi, T., Okuyama, K., Oike, Y. and Yamamura, K. (1997). Efficiency of recombination by Cre transient expression in embryonic stem cells: comparison of various promoters. *J Biochem* **122**, 977-982.

Attardi, A., Fulton, T., Florescu, M., Shah, G., Muresan, L., Lenz, M. O., Lancaster, C., Huisken, J., van Oudenaarden, A. and Steventon, B. (2018). Neuromesodermal progenitors are a conserved source of spinal cord with divergent growth dynamics. *Development* **145**.

Baillie-Johnson, P., Voiculescu, O., Hayward, P. and Steventon, B. (2018). The Chick Caudolateral Epiblast Acts as a Permissive Niche for Generating Neuromesodermal Progenitor Behaviours. *Cells Tissues Organs* **205**, 320-330.

Beccari, L., Moris, N., Girgin, M., Turner, D. A., Baillie-Johnson, P., Cossy, A. C., Lutolf, M. P., Duboule, D. and Arias, A. M. (2018). Multi-axial self-organization properties of mouse embryonic stem cells into gastruloids. *Nature* **562**, 272-276.

Beck, C. W. and Slack, J. M. (1998). Analysis of the developing Xenopus tail bud reveals separate phases of gene expression during determination and outgrowth. *Mech Dev* **72**, 41-52.

Beck, C. W. and Slack, J. M. (1999). A developmental pathway controlling outgrowth of the Xenopus tail bud. *Development* **126**, 1611-1620.

Bellomo, D., Lander, A., Harragan, I. and Brown, N. A. (1996). Cell proliferation in mammalian gastrulation: the ventral node and notochord are relatively quiescent. *Dev Dyn* **205**, 471-485.

Bialecka, M., Wilson, V. and Deschamps, J. (2010). Cdx mutant axial progenitor cells are rescued by grafting to a wild type environment. *Dev Biol* **347**, 228-234.

Bouldin, C. M., Manning, A. J., Peng, Y. H., Farr, G. H., 3rd, Hung, K. L., Dong, A. and Kimelman, D. (2015). Wnt signaling and tbx16 form a bistable switch to commit bipotential progenitors to mesoderm. *Development* **142**, 2499-2507.

Boulet, A. M. and Capecchi, M. R. (2012). Signaling by FGF4 and FGF8 is required for axial elongation of the mouse embryo. *Dev Biol* **371**, 235-245.

Brown, J. M. and Storey, K. G. (2000). A region of the vertebrate neural plate in which neighbouring cells can adopt neural or epidermal fates. *Curr Biol* **10**, 869-872.

Bulusu, V., Prior, N., Snaebjornsson, M. T., Kuehne, A., Sonnen, K. F., Kress, J., Stein, F., Schultz, C., Sauer, U. and Aulehla, A. (2017). Spatiotemporal Analysis of a Glycolytic Activity Gradient Linked to Mouse Embryo Mesoderm Development. *Dev Cell* **40**, 331-341 e334.

Burke, A. C., Nelson, C. E., Morgan, B. A. and Tabin, C. (1995). Hox genes and the evolution of vertebrate axial morphology. *Development* **121**, 333-346.

Cambray, N. and Wilson, V. (2002). Axial progenitors with extensive potency are localised to the mouse chordoneural hinge. *Development* **129**, 4855-4866.

Cambray, N. and Wilson, V. (2007). Two distinct sources for a population of maturing axial progenitors. *Development* **134**, 2829-2840.

Carter, T. C., Pangilinan, F., Troendle, J. F., Molloy, A. M., VanderMeer, J., Mitchell, A., Kirke, P. N., Conley, M. R., Shane, B., Scott, J. M., et al. (2011). Evaluation of 64 candidate single nucleotide polymorphisms as risk factors for neural tube defects in a large Irish study population. *Am J Med Genet A* **155A**, 14-21.

Catala, M., Teillet, M. A. and Le Douarin, N. M. (1995). Organization and development of the tail bud analyzed with the quail-chick chimaera system. *Mech Dev* **51**, 51-65.

Chal, J., Al Tanoury, Z., Hestin, M., Gobert, B., Aivio, S., Hick, A., Cherrier, T., Nesmith, A. P., Parker, K. K. and Pourquie, O. (2016). Generation of human muscle fibers and satellite-like cells from human pluripotent stem cells in vitro. *Nat Protoc* **11**, 1833-1850.

Chalamalasetty, R. B., Dunty, W. C., Jr., Biris, K. K., Ajima, R., Iacovino, M., Beisaw, A., Feigenbaum, L., Chapman, D. L., Yoon, J. K., Kyba, M., et al. (2011). The Wnt3a/beta-catenin target gene Mesogenin1 controls the segmentation clock by activating a Notch signalling program. *Nat Commun* **2**, 390.

Chalamalasetty, R. B., Garriock, R. J., Dunty, W. C., Jr., Kennedy, M. W., Jailwala, P., Si, H. and Yamaguchi, T. P. (2014). Mesogenin 1 is a master regulator of paraxial presomitic mesoderm differentiation. *Development* **141**, 4285-4297.

Chambers, S. M., Fasano, C. A., Papapetrou, E. P., Tomishima, M., Sadelain, M. and Studer, L. (2009). Highly efficient neural conversion of human ES and iPS cells by dual inhibition of SMAD signaling. *Nat Biotechnol* **27**, 275-280.

Chan, B. W., Chan, K. S., Koide, T., Yeung, S. M., Leung, M. B., Copp, A. J., Loeken, M. R., Shiroishi, T. and Shum, A. S. (2002). Maternal diabetes increases the risk of caudal regression caused by retinoic acid. *Diabetes* **51**, 2811-2816.

Choi, H. M. T., Schwarzkopf, M., Fornace, M. E., Acharya, A., Artavanis, G., Stegmaier, J., Cunha, A. and Pierce, N. A. (2018). Third-generation in situ hybridization chain reaction: multiplexed, quantitative, sensitive, versatile, robust. *Development* **145**.

Cooper, F., Gentsch, G. E., Mitter, E., Bouissou, C., Healy, L., Hernandez-Rodriguez, A., Smith, J. C. and Bernardo, A. S. (2020). Rostrocaudal Patterning and Neural Crest Differentiation of Human Pre-Neural Spinal Cord Progenitors in vitro. *bioRxiv*.

Cunningham, T. J., Colas, A. and Duester, G. (2016). Early molecular events during retinoic acid induced differentiation of neuromesodermal progenitors. *Biol Open* **5**, 1821-1833.

Cunningham, T. J., Kumar, S., Yamaguchi, T. P. and Duester, G. (2015). Wnt8a and Wnt3a cooperate in the axial stem cell niche to promote mammalian body axis extension. *Dev Dyn* **244**, 797-807.

Cunningham, T. J., Zhao, X. and Duester, G. (2011). Uncoupling of retinoic acid signaling from tailbud development before termination of body axis extension. *Genesis* **49**, 776-783.

Dady, A., Havis, E., Escriou, V., Catala, M. and Duband, J. L. (2014). Junctional neurulation: a unique developmental program shaping a discrete region of the spinal cord highly susceptible to neural tube defects. *J Neurosci* **34**, 13208-13221.

Davis, R. L. and Kirschner, M. W. (2000). The fate of cells in the tailbud of Xenopus laevis. *Development* **127**, 255-267.

de Lemos, L., Nóvoa, A. and Mallo, M. (2019). High Epha1 expression is a potential cell surface marker for embryonic neuro-mesodermal progenitors. *bioRxiv*.

Delfino-Machin, M., Lunn, J. S., Breitkreuz, D. N., Akai, J. and Storey, K. G. (2005). Specification and maintenance of the spinal cord stem zone. *Development* **132**, 4273-4283.

Denans, N., Iimura, T. and Pourquie, O. (2015). Hox genes control vertebrate body elongation by collinear Wnt repression. *Elife* **4**.

Denham, M., Hasegawa, K., Menheniott, T., Rollo, B., Zhang, D., Hough, S., Alshawaf, A., Febbraro, F., Ighaniyan, S., Leung, J., et al. (2015). Multipotent caudal neural progenitors derived from human pluripotent stem cells that give rise to lineages of the central and peripheral nervous system. *Stem Cells* **33**, 1759-1770.

Deschamps, J. and van Nes, J. (2005). Developmental regulation of the Hox genes during axial morphogenesis in the mouse. *Development* **132**, 2931-2942.

DeVeale, B., Brokhman, I., Mohseni, P., Babak, T., Yoon, C., Lin, A., Onishi, K., Tomilin, A., Pevny, L., Zandstra, P. W., et al. (2013). Oct4 is required ~E7.5 for proliferation in the primitive streak. *PLoS Genet* **9**, e1003957.

Dias, A., Lozovska, A., Wymeersch, F. J., Novoa, A., Binagui-Casas, A., Sobral, D., Martins, G. G., Wilson, V. and Mallo, M. (2020). A Tgfbr1/Snai1-dependent developmental module at the core of vertebrate axial elongation. *Elife* **9**.

Diaz-Cuadros, M., Wagner, D. E., Budjan, C., Hubaud, A., Tarazona, O. A., Donelly, S., Michaut, A., Al Tanoury, Z., Yoshioka-Kobayashi, K., Niino, Y., et al. (2020). In vitro characterization of the human segmentation clock. *Nature*.

Diez del Corral, R., Breitkreuz, D. N. and Storey, K. G. (2002). Onset of neuronal differentiation is regulated by paraxial mesoderm and requires attenuation of FGF signalling. *Development* **129**, 1681-1691.

Diez del Corral, R., Olivera-Martinez, I., Goriely, A., Gale, E., Maden, M. and Storey, K. (2003). Opposing FGF and retinoid pathways control ventral neural pattern, neuronal differentiation, and segmentation during body axis extension. *Neuron* **40**, 65-79.

Dunty, W. C., Jr., Biris, K. K., Chalamalasetty, R. B., Taketo, M. M., Lewandoski, M. and Yamaguchi, T. P. (2008). Wnt3a/beta-catenin signaling controls posterior body development by coordinating mesoderm formation and segmentation. *Development* **135**, 85-94.

Dunty, W. C., Jr., Kennedy, M. W., Chalamalasetty, R. B., Campbell, K. and Yamaguchi, T. P. (2014). Transcriptional profiling of Wnt3a mutants identifies Sp transcription factors as essential effectors of the Wnt/beta-catenin pathway in neuromesodermal stem cells. *PLoS One* **9**, e87018.

Duval, N., Vaslin, C., Barata, T., Frarma, Y., Contremoulins, V., Baudin, X., Nedelec, S. and Ribes, V. (2019). BMP4 patterns Smad activity and generates stereotyped cell fate organisation in spinal organoids. *Development*.

Economides, K. D., Zeltser, L. and Capecchi, M. R. (2003). Hoxb13 mutations cause overgrowth of caudal spinal cord and tail vertebrae. *Dev Biol* **256**, 317-330.

Economou, C., Tsakiridis, A., Wymeersch, F. J., Gordon-Keylock, S., Dewhurst, R. E., Fisher, D., Medvinsky, A., Smith, A. J. and Wilson, V. (2015). Intrinsic factors and the embryonic environment influence the formation of extragonadal teratomas during gestation. *BMC Dev Biol* **15**, 35.

Edri, S., Hayward, P., Baillie-Johnson, P., Steventon, B. J. and Martinez Arias, A. (2019a). An epiblast stem cell-derived multipotent progenitor population for axial extension. *Development* **146**.

Edri, S., Hayward, P., Jawaid, W. and Martinez Arias, A. (2019b). Neuro-mesodermal progenitors (NMPs): a comparative study between pluripotent stem cells and embryo-derived populations. *Development* **146**.

Eng, C. L., Lawson, M., Zhu, Q., Dries, R., Koulena, N., Takei, Y., Yun, J., Cronin, C., Karp, C., Yuan, G. C., et al. (2019). Transcriptome-scale super-resolved imaging in tissues by RNA seqFISH. *Nature* **568**, 235-239.

Faustino Martins, J. M., Fischer, C., Urzi, A., Vidal, R., Kunz, S., Ruffault, P. L., Kabuss, L., Hube, I., Gazzerro, E., Birchmeier, C., et al. (2020). Self-Organizing 3D Human Trunk Neuromuscular Organoids. *Cell Stem Cell* **26**, 172-186 e176.

Fellous, M., Boue, J., Malbrunot, C., Wollman, E., Sasportes, M., Van Cong, N., Marcelli, A., Rebourcet, R., Hubert, C., Demenais, F., et al. (1982). A five-generation family with sacral agenesis and spina bifida: possible similarities with the mouse T-locus. *Am J Med Genet* **12**, 465-487.

Forlani, S., Lawson, K. A. and Deschamps, J. (2003). Acquisition of Hox codes during gastrulation and axial elongation in the mouse embryo. *Development* **130**, 3807-3819.

Frith, T. J., Granata, I., Wind, M., Stout, E., Thompson, O., Neumann, K., Stavish, D., Heath, P. R., Ortmann, D., Hackland, J. O., et al. (2018). Human axial progenitors generate trunk neural crest cells in vitro. *Elife* **7**.

Frith, T. J. R. and Tsakiridis, A. (2019). Efficient Generation of Trunk Neural Crest and Sympathetic Neurons from Human Pluripotent Stem Cells Via a Neuromesodermal Axial Progenitor Intermediate. *Curr Protoc Stem Cell Biol* **49**, e81.

Galceran, J., Farinas, I., Depew, M. J., Clevers, H. and Grosschedl, R. (1999). Wnt3a-/--like phenotype and limb deficiency in Lef1(-/-)Tcf1(-/-) mice. *Genes Dev* **13**, 709-717.

Galea, G. L., Cho, Y. J., Galea, G., Mole, M. A., Rolo, A., Savery, D., Moulding, D., Culshaw, L. H., Nikolopoulou, E., Greene, N. D. E., et al. (2017). Biomechanical coupling facilitates spinal neural tube closure in mouse embryos. *Proc Natl Acad Sci U S A* **114**, E5177-E5186.

Garriock, R. J., Chalamalasetty, R. B., Kennedy, M. W., Canizales, L. C., Lewandoski, M. and Yamaguchi, T. P. (2015). Lineage tracing of neuromesodermal progenitors reveals novel Wnt-dependent roles in trunk progenitor cell maintenance and differentiation. *Development* **142**, 1628-1638.

Gentsch, G. E., Owens, N. D., Martin, S. R., Piccinelli, P., Faial, T., Trotter, M. W., Gilchrist, M. J. and Smith, J. C. (2013). In vivo T-box transcription factor profiling reveals joint regulation of embryonic neuromesodermal bipotency. *Cell Rep* **4**, 1185-1196.

Ghebranious, N., Blank, R. D., Raggio, C. L., Staubli, J., McPherson, E., Ivacic, L., Rasmussen, K., Jacobsen, F. S., Faciszewski, T., Burmester, J. K., et al. (2008). A missense T (Brachyury) mutation contributes to vertebral malformations. *J Bone Miner Res* **23**, 1576-1583.

Gomez, C., Ozbudak, E. M., Wunderlich, J., Baumann, D., Lewis, J. and Pourquie, O. (2008). Control of segment number in vertebrate embryos. *Nature* **454**, 335-339.

Gomez, G. A., Prasad, M.S., Wong, M., Cherney, R.M., Shelar, P.B., Sandhu, N., Hackland, J.O.S., Hernandez, J.C., Leung, A.W. and Garcia, M.I. (2019). WNT/β-CATENIN modulates the axial identity of ES derived human neural crest.

Gont, L. K., Steinbeisser, H., Blumberg, B. and de Robertis, E. M. (1993). Tail formation as a continuation of gastrulation: the multiple cell populations of the Xenopus tailbud derive from the late blastopore lip. *Development* **119**, 991-1004.

Gordon, C. T., Attanasio, C., Bhatia, S., Benko, S., Ansari, M., Tan, T. Y., Munnich, A., Pennacchio, L. A., Abadie, V., Temple, I. K., et al. (2014). Identification of novel craniofacial regulatory domains located far upstream of SOX9 and disrupted in Pierre Robin sequence. *Hum Mutat* **35**, 1011-1020.

Goto, H., Kimmey, S. C., Row, R. H., Matus, D. Q. and Martin, B. L. (2017). FGF and canonical Wnt signaling cooperate to induce paraxial mesoderm from tailbud neuromesodermal progenitors through regulation of a two-step epithelial to mesenchymal transition. *Development* **144**, 1412-1424.

Gouti, M., Delile, J., Stamataki, D., Wymeersch, F. J., Huang, Y., Kleinjung, J., Wilson, V. and Briscoe, J. (2017). A Gene Regulatory Network Balances Neural and Mesoderm Specification during Vertebrate Trunk Development. *Dev Cell* **41**, 243-261 e247.

Gouti, M., Tsakiridis, A., Wymeersch, F. J., Huang, Y., Kleinjung, J., Wilson, V. and Briscoe, J. (2014). In vitro generation of neuromesodermal progenitors reveals distinct roles for wnt signalling in the specification of spinal cord and paraxial mesoderm identity. *PLoS Biol* **12**, e1001937.

Guillot, C., Michaut, A., Rabe, B. and Pourquié, O. (2020). Dynamics of primitive streak regression controls the fate of neuro-mesodermal progenitors in the chicken embryo. *bioRxiv*.

Hackland, J. O. S., Frith, T. J. R., Thompson, O., Marin Navarro, A., Garcia-Castro, M. I., Unger, C. and Andrews, P. W. (2017). Top-Down Inhibition of BMP Signaling Enables Robust Induction of hPSCs Into Neural Crest in Fully Defined, Xeno-free Conditions. *Stem Cell Reports* **9**, 1043-1052.

Hackland, J. O. S., Shelar, P. B., Sandhu, N., Prasad, M. S., Charney, R. M., Gomez, G. A., Frith, T. J. R. and Garcia-Castro, M. I. (2019). FGF Modulates the Axial Identity of Trunk hPSC-Derived Neural Crest but Not the Cranial-Trunk Decision. *Stem Cell Reports* **12**, 920-933.

Henrique, D., Abranches, E., Verrier, L. and Storey, K. G. (2015). Neuromesodermal progenitors and the making of the spinal cord. *Development* **142**, 2864-2875.

Hofmann, M., Schuster-Gossler, K., Watabe-Rudolph, M., Aulehla, A., Herrmann, B. G. and Gossler, A. (2004). WNT signaling, in synergy with T/TBX6, controls Notch signaling by regulating Dll1 expression in the presomitic mesoderm of mouse embryos. *Genes Dev* **18**, 2712-2717.

Huang, Y., Osorno, R., Tsakiridis, A. and Wilson, V. (2012). In Vivo differentiation potential of epiblast stem cells revealed by chimeric embryo formation. *Cell Rep* **2**, 1571-1578.

Iimura, T., Yang, X., Weijer, C. J. and Pourquie, O. (2007). Dual mode of paraxial mesoderm formation during chick gastrulation. *Proc Natl Acad Sci U S A* **104**, 2744-2749.

Imaizumi, K., Sone, T., Ibata, K., Fujimori, K., Yuzaki, M., Akamatsu, W. and Okano, H. (2015). Controlling the Regional Identity of hPSC-Derived Neurons to Uncover Neuronal Subtype Specificity of Neurological Disease Phenotypes. *Stem Cell Reports* **5**, 1010-1022.

Javali, A., Misra, A., Leonavicius, K., Acharyya, D., Vyas, B. and Sambasivan, R. (2017). Co-expression of Tbx6 and Sox2 identifies a novel transient neuromesoderm progenitor cell state. *Development* **144**, 4522-4529.

Jensen, L. E., Barbaux, S., Hoess, K., Fraterman, S., Whitehead, A. S. and Mitchell, L. E. (2004). The human T locus and spina bifida risk. *Hum Genet* **115**, 475-482.

Junker, J. P., Noel, E. S., Guryev, V., Peterson, K. A., Shah, G., Huisken, J., McMahon, A. P., Berezikov, E., Bakkers, J. and van Oudenaarden, A. (2014). Genome-wide RNA Tomography in the zebrafish embryo. *Cell* **159**, 662-675.

Jurberg, A. D., Aires, R., Novoa, A., Rowland, J. E. and Mallo, M. (2014). Compartment-dependent activities of Wnt3a/beta-catenin signaling during vertebrate axial extension. *Dev Biol* **394**, 253-263.

Jurberg, A. D., Aires, R., Varela-Lasheras, I., Novoa, A. and Mallo, M. (2013). Switching axial progenitors from producing trunk to tail tissues in vertebrate embryos. *Dev Cell* **25**, 451-462.

Kadoya, K., Lu, P., Nguyen, K., Lee-Kubli, C., Kumamaru, H., Yao, L., Knackert, J., Poplawski, G., Dulin, J. N., Strobl, H., et al. (2016). Spinal cord reconstitution with homologous neural grafts enables robust corticospinal regeneration. *Nat Med* **22**, 479-487.

Kanki, J. P. and Ho, R. K. (1997). The development of the posterior body in zebrafish. *Development* **124**, 881-893.

Kennedy, M. W., Chalamalasetty, R. B., Thomas, S., Garriock, R. J., Jailwala, P. and Yamaguchi, T. P. (2016). Sp5 and Sp8 recruit beta-catenin and Tcf1-Lef1 to select enhancers to activate Wnt target gene transcription. *Proc Natl Acad Sci U S A* **113**, 3545-3550.

Kimmel, C. B., Ballard, W. W., Kimmel, S. R., Ullmann, B. and Schilling, T. F. (1995). Stages of embryonic development of the zebrafish. *Dev Dyn* **203**, 253-310.

Kimmel, C. B., Warga, R. M. and Schilling, T. F. (1990). Origin and organization of the zebrafish fate map. *Development* **108**, 581-594.

Kinder, S. J., Tsang, T. E., Quinlan, G. A., Hadjantonakis, A. K., Nagy, A. and Tam, P. P. (1999). The orderly allocation of mesodermal cells to the extraembryonic structures and the anteroposterior axis during gastrulation of the mouse embryo. *Development* **126**, 4691-4701.

Kirino, K., Nakahata, T., Taguchi, T. and Saito, M. K. (2018). Efficient derivation of sympathetic neurons from human pluripotent stem cells with a defined condition. *Sci Rep* **8**, 12865.

Kirkeby, A., Grealish, S., Wolf, D. A., Nelander, J., Wood, J., Lundblad, M., Lindvall, O. and Parmar, M. (2012). Generation of regionally specified neural progenitors and functional neurons from human embryonic stem cells under defined conditions. *Cell Rep* **1**, 703-714.

Knight, G. T., Lundin, B. F., Iyer, N., Ashton, L. M., Sethares, W. A., Willett, R. M. and Ashton, R. S. (2018). Engineering induction of singular neural rosette emergence within hPSC-derived tissues. *Elife* **7**.

Koch, F., Scholze, M., Wittler, L., Schifferl, D., Sudheer, S., Grote, P., Timmermann, B., Macura, K. and Herrmann, B. G. (2017). Antagonistic Activities of Sox2 and Brachyury Control the Fate Choice of Neuro-Mesodermal Progenitors. *Dev Cell* **42**, 514-526 e517.

Kumamaru, H., Kadoya, K., Adler, A. F., Takashima, Y., Graham, L., Coppola, G. and Tuszynski, M. H. (2018). Generation and post-injury integration of human spinal cord neural stem cells. *Nat Methods* **15**, 723-731.

Kumar, S. and Duester, G. (2014). Retinoic acid controls body axis extension by directly repressing Fgf8 transcription. *Development* **141**, 2972-2977.

Kuratani, S. (2009). Modularity, comparative embryology and evo-devo: developmental dissection of evolving body plans. *Dev Biol* **332**, 61-69.

Lauschke, V. M., Tsiairis, C. D., Francois, P. and Aulehla, A. (2013). Scaling of embryonic patterning based on phase-gradient encoding. *Nature* **493**, 101-105.

Lawson, K. A., Meneses, J. J. and Pedersen, R. A. (1991). Clonal analysis of epiblast fate during germ layer formation in the mouse embryo. *Development* **113**, 891-911.

Lee, G., Kim, H., Elkabetz, Y., Al Shamy, G., Panagiotakos, G., Barberi, T., Tabar, V. and Studer, L. (2007). Isolation and directed differentiation of neural crest stem cells derived from human embryonic stem cells. *Nat Biotechnol* **25**, 1468-1475.

Li, X., Yue, X., Pastor, W. A., Lin, L., Georges, R., Chavez, L., Evans, S. M. and Rao, A. (2016). Tet proteins influence the balance between neuroectodermal and mesodermal fate choice by inhibiting Wnt signaling. *Proc Natl Acad Sci U S A* **113**, E8267-E8276.

Libby, A. R. G., Joy, D.A., Elder, N.H., Bulger, E.A., Krakora, M.Z., Gaylord, E.A., Mendoza-Camacho, F., and McDevitt, T.C. (2020). Axial Elongation of Caudalized Human Pluripotent Stem Cell Organoids Mimics Neural Tube Development. *bioRxiv*.

Lippmann, E. S., Williams, C. E., Ruhl, D. A., Estevez-Silva, M. C., Chapman, E. R., Coon, J. J. and Ashton, R. S. (2015). Deterministic HOX patterning in human pluripotent stem cell-derived neuroectoderm. *Stem Cell Reports* **4**, 632-644.

Liu, J. P., Laufer, E. and Jessell, T. M. (2001). Assigning the positional identity of spinal motor neurons: rostrocaudal patterning of Hox-c expression by FGFs, Gdf11, and retinoids. *Neuron* **32**, 997-1012.

Liu, Y., Sugiyama, F., Yagami, K. and Ohkawa, H. (2003). Sharing of the same embryogenic pathway in anorectal malformations and anterior sacral myelomeningocele formation. *Pediatr Surg Int* **19**, 152-156.

Livigni, A., Peradziryi, H., Sharov, A. A., Chia, G., Hammachi, F., Migueles, R. P., Sukparangsi, W., Pernagallo, S., Bradley, M., Nichols, J., et al. (2013). A conserved Oct4/POUV-dependent network links adhesion and migration to progenitor maintenance. *Curr Biol* **23**, 2233-2244.

Loh, K. M., Chen, A., Koh, P. W., Deng, T. Z., Sinha, R., Tsai, J. M., Barkal, A. A., Shen, K. Y., Jain, R., Morganti, R. M., et al. (2016). Mapping the Pairwise Choices Leading from Pluripotency to Human Bone, Heart, and Other Mesoderm Cell Types. *Cell* **166**, 451-467.

Lolas, M., Valenzuela, P. D., Tjian, R. and Liu, Z. (2014). Charting Brachyury-mediated developmental pathways during early mouse embryogenesis. *Proc Natl Acad Sci U S A* **111**, 4478-4483.

Lopez-Escobar, B., Caro-Vega, J. M., Vijayraghavan, D. S., Plageman, T. F., Sanchez-Alcazar, J. A., Moreno, R. C., Savery, D., Marquez-Rivas, J., Davidson, L. A. and Ybot-Gonzalez, P. (2018). The non-canonical Wnt-PCP pathway shapes the mouse caudal neural plate. *Development* **145**.

Mallo, M., Wellik, D. M. and Deschamps, J. (2010). Hox genes and regional patterning of the vertebrate body plan. *Dev Biol* **344**, 7-15.

Martin, B. L. and Kimelman, D. (2008). Regulation of canonical Wnt signaling by Brachyury is essential for posterior mesoderm formation. *Dev Cell* **15**, 121-133.

Martin, B. L. and Kimelman, D. (2010). Brachyury establishes the embryonic mesodermal progenitor niche. *Genes Dev* **24**, 2778-2783.

Martin, B. L. and Kimelman, D. (2012). Canonical Wnt signaling dynamically controls multiple stem cell fate decisions during vertebrate body formation. *Dev Cell* **22**, 223-232.

Martinez Arias, A. and Steventon, B. (2018). On the nature and function of organizers. *Development* **145**.

Mastromina, I., Verrier, L., Silva, J. C., Storey, K. G. and Dale, J. K. (2018). Myc activity is required for maintenance of the neuromesodermal progenitor signalling network and for segmentation clock gene oscillations in mouse. *Development* **145**.

Mathis, L. and Nicolas, J. F. (2000). Different clonal dispersion in the rostral and caudal mouse central nervous system. *Development* **127**, 1277-1290.

Matsubara, Y., Hirasawa, T., Egawa, S., Hattori, A., Suganuma, T., Kohara, Y., Nagai, T., Tamura, K., Kuratani, S., Kuroiwa, A., et al. (2017). Anatomical integration of the sacral-hindlimb unit coordinated by GDF11 underlies variation in hindlimb positioning in tetrapods. *Nat Ecol Evol* **1**, 1392-1399.

Matsuda, M., Yamanaka, Y., Uemura, M., Osawa, M., Saito, M. K., Nagahashi, A., Nishio, M., Guo, L., Ikegawa, S., Sakurai, S., et al. (2020). Recapitulating the human segmentation clock with pluripotent stem cells. *Nature* **580**, 124-129.

Maury, Y., Come, J., Piskorowski, R. A., Salah-Mohellibi, N., Chevaleyre, V., Peschanski, M., Martinat, C. and Nedelec, S. (2015). Combinatorial analysis of developmental cues efficiently converts human pluripotent stem cells into multiple neuronal subtypes. *Nat Biotechnol* **33**, 89-96.

Mazzoni, E. O., Mahony, S., Peljto, M., Patel, T., Thornton, S. R., McCuine, S., Reeder, C., Boyer, L. A., Young, R. A., Gifford, D. K., et al. (2013). Saltatory remodeling of Hox chromatin in response to rostrocaudal patterning signals. *Nat Neurosci* **16**, 1191-1198.

McGrew, M. J., Sherman, A., Lillico, S. G., Ellard, F. M., Radcliffe, P. A., Gilhooley, H. J., Mitrophanous, K. A., Cambray, N., Wilson, V. and Sang, H. (2008). Localised axial progenitor cell populations in the avian tail bud are not committed to a posterior Hox identity. *Development* **135**, 2289-2299.

Meinhardt, A., Eberle, D., Tazaki, A., Ranga, A., Niesche, M., Wilsch-Brauninger, M., Stec, A., Schackert, G., Lutolf, M. and Tanaka, E. M. (2014). 3D reconstitution of the patterned neural tube from embryonic stem cells. *Stem Cell Reports* **3**, 987-999.

Menendez, L., Yatskievych, T. A., Antin, P. B. and Dalton, S. (2011). Wnt signaling and a Smad pathway blockade direct the differentiation of human pluripotent stem cells to multipotent neural crest cells. *Proc Natl Acad Sci U S A* **108**, 19240-19245.

Metzis, V., Steinhauser, S., Pakanavicius, E., Gouti, M., Stamataki, D., Ivanovitch, K., Watson, T., Rayon, T., Mousavy Gharavy, S. N., Lovell-Badge, R., et al. (2018). Nervous System Regionalization Entails Axial Allocation before Neural Differentiation. *Cell* **175**, 1105-1118 e1117.

Miura, S., Davis, S., Klingensmith, J. and Mishina, Y. (2006). BMP signaling in the epiblast is required for proper recruitment of the prospective paraxial mesoderm and development of the somites. *Development* **133**, 3767-3775.

Molotkova, N., Molotkov, A., Sirbu, I. O. and Duester, G. (2005). Requirement of mesodermal retinoic acid generated by Raldh2 for posterior neural transformation. *Mech Dev* **122**, 145-155.

Mongera, A., Rowghanian, P., Gustafson, H. J., Shelton, E., Kealhofer, D. A., Carn, E. K., Serwane, F., Lucio, A. A., Giammona, J. and Campas, O. (2018). A fluid-to-solid jamming transition underlies vertebrate body axis elongation. *Nature* **561**, 401-405.

Morrison, K., Papapetrou, C., Attwood, J., Hol, F., Lynch, S. A., Sampath, A., Hamel, B., Burn, J., Sowden, J., Stott, D., et al. (1996). Genetic mapping of the human homologue (T) of mouse T(Brachyury) and a search for allele association between human T and spina bifida. *Hum Mol Genet* **5**, 669-674.

Mouilleau, V., Vaslin, C., Gribaudo, S., Robert, R., Nicolas, N., Jarrige, M., Terray, A., Lesueur, L., Mathis, M. W., Croft, G., Daynac, M., Rouiller-Fabre, V., Wichterle, H., Ribes, V., Martinat, C. and Nedelec, S. (2020). Dynamic extrinsic pacing of the HOX clock in human axial progenitors controls motor neuron subtype specification. *bioRxiv*.

Mugele, D., Moulding, D.A., Savery, D., Mole, M.A., Greene, N.D.A., Martinez-Barbera, J.P. and Copp, A.J. (2018). Genetic approaches in mice demonstrate that neuro-mesodermal progenitors express T/Brachyury but not Sox2. *bioRxiv*.

Muller, F. and O'Rahilly, R. (2004). The primitive streak, the caudal eminence and related structures in staged human embryos. *Cells Tissues Organs* **177**, 2-20.

Nakashima, M., Toyono, T., Akamine, A. and Joyner, A. (1999). Expression of growth/differentiation factor 11, a new member of the BMP/TGFbeta superfamily during mouse embryogenesis. *Mech Dev* **80**, 185-189.

Neijts, R., Amin, S., van Rooijen, C. and Deschamps, J. (2017). Cdx is crucial for the timing mechanism driving colinear Hox activation and defines a trunk segment in the Hox cluster topology. *Dev Biol* **422**, 146-154.

Nicolas, J. F., Mathis, L., Bonnerot, C. and Saurin, W. (1996). Evidence in the mouse for self-renewing stem cells in the formation of a segmented longitudinal structure, the myotome. *Development* **122**, 2933-2946.

Nieuwkoop, P. D. and Nigtevecht, G. V. (1954). Neural Activation and Transformation in Explants of Competent Ectoderm under the Influence of Fragments of Anterior Notochord in Urodeles. *J Embryol Exp Morph* **2**, 175-193.

Nordstrom, U., Maier, E., Jessell, T. M. and Edlund, T. (2006). An early role for WNT signaling in specifying neural patterns of Cdx and Hox gene expression and motor neuron subtype identity. *PLoS Biol* **4**, e252.

Oginuma, M., Moncuquet, P., Xiong, F., Karoly, E., Chal, J., Guevorkian, K. and Pourquie, O. (2017). A Gradient of Glycolytic Activity Coordinates FGF and Wnt Signaling during Elongation of the Body Axis in Amniote Embryos. *Dev Cell* **40**, 342-353 e310.

Olivera-Martinez, I., Harada, H., Halley, P. A. and Storey, K. G. (2012). Loss of FGF-dependent mesoderm identity and rise of endogenous retinoid signalling determine cessation of body axis elongation. *PLoS Biol* **10**, e1001415.

Olivera-Martinez, I., Schurch, N., Li, R. A., Song, J., Halley, P. A., Das, R. M., Burt, D. W., Barton, G. J. and Storey, K. G. (2014). Major transcriptome re-organisation and abrupt changes in signalling, cell cycle and chromatin regulation at neural differentiation in vivo. *Development* **141**, 3266-3276.

Olivera-Martinez, I. and Storey, K. G. (2007). Wnt signals provide a timing mechanism for the FGF-retinoid differentiation switch during vertebrate body axis extension. *Development* **134**, 2125-2135.

Osorno, R., Tsakiridis, A., Wong, F., Cambray, N., Economou, C., Wilkie, R., Blin, G., Scotting, P. J., Chambers, I. and Wilson, V. (2012). The developmental dismantling of pluripotency is reversed by ectopic Oct4 expression. *Development* **139**, 2288-2298.

Padmanabhan, R. (1998). Retinoic acid-induced caudal regression syndrome in the mouse fetus. *Reprod Toxicol* **12**, 139-151.

Peljto, M., Dasen, J. S., Mazzoni, E. O., Jessell, T. M. and Wichterle, H. (2010). Functional diversity of ESC-derived motor neuron subtypes revealed through intraspinal transplantation. *Cell Stem Cell* **7**, 355-366.

Perantoni, A. O., Timofeeva, O., Naillat, F., Richman, C., Pajni-Underwood, S., Wilson, C., Vainio, S., Dove, L. F. and Lewandoski, M. (2005). Inactivation of FGF8 in early mesoderm reveals an essential role in kidney development. *Development* **132**, 3859-3871.

Postma, A. V., Alders, M., Sylva, M., Bilardo, C. M., Pajkrt, E., van Rijn, R. R., Schulte-Merker, S., Bulk, S., Stefanovic, S., Ilgun, A., et al. (2014). Mutations in the T (brachyury) gene cause a novel syndrome consisting of sacral agenesis, abnormal ossification of the vertebral bodies and a persistent notochordal canal. *J Med Genet* **51**, 90-97.

Qian, L., Mahaffey, J. P., Alcorn, H. L. and Anderson, K. V. (2011). Tissue-specific roles of Axin2 in the inhibition and activation of Wnt signaling in the mouse embryo. *Proc Natl Acad Sci U S A* **108**, 8692-8697.

Rashbass, P., Wilson, V., Rosen, B. and Beddington, R. S. (1994). Alterations in gene expression during mesoderm formation and axial patterning in Brachyury (T) embryos. *Int J Dev Biol* **38**, 35-44.

Ribes, V., Le Roux, I., Rhinn, M., Schuhbaur, B. and Dolle, P. (2009). Early mouse caudal development relies on crosstalk between retinoic acid, Shh and Fgf signalling pathways. *Development* **136**, 665-676.

Robinton, D. A., Chal, J., Lummertz da Rocha, E., Han, A., Yermalovich, A. V., Oginuma, M., Schlaeger, T. M., Sousa, P., Rodriguez, A., Urbach, A., et al. (2019). The Lin28/let-7 Pathway Regulates the Mammalian Caudal Body Axis Elongation Program. *Dev Cell* **48**, 396-405 e393.

Rocha, P. P., Scholze, M., Bleiss, W. and Schrewe, H. (2010). Med12 is essential for early mouse development and for canonical Wnt and Wnt/PCP signaling. *Development* **137**, 2723-2731.

Rodrigo Albors, A., Halley, P. A. and Storey, K. G. (2018). Lineage tracing of axial progenitors using Nkx1-2CreER(T2) mice defines their trunk and tail contributions. *Development* **145**.

Rodriques, S. G., Stickels, R. R., Goeva, A., Martin, C. A., Murray, E., Vanderburg, C. R., Welch, J., Chen, L. M., Chen, F. and Macosko, E. Z. (2019). Slide-seq: A scalable technology for measuring genome-wide expression at high spatial resolution. *Science* **363**, 1463-1467.

Row, R. H., Pegg, A., Kinney, B. A., Farr, G. H., 3rd, Maves, L., Lowell, S., Wilson, V. and Martin, B. L. (2018). BMP and FGF signaling interact to pattern mesoderm by controlling basic helix-loop-helix transcription factor activity. *Elife* **7**.

Rulle, A., Tsikolia, N., de Bakker, B., Drummer, C., Behr, R. and Viebahn, C. (2018). On the Enigma of the Human Neurenteric Canal. *Cells Tissues Organs* **205**, 256-278.

Sakai, Y., Meno, C., Fujii, H., Nishino, J., Shiratori, H., Saijoh, Y., Rossant, J. and Hamada, H. (2001). The retinoic acid-inactivating enzyme CYP26 is essential for establishing an uneven distribution of retinoic acid along the anterio-posterior axis within the mouse embryo. *Genes Dev* **15**, 213-225.

Savory, J. G., Bouchard, N., Pierre, V., Rijli, F. M., De Repentigny, Y., Kothary, R. and Lohnes, D. (2009). Cdx2 regulation of posterior development through non-Hox targets. *Development* **136**, 4099-4110.

Schmidt, C., Wilson, V., Stott, D. and Beddington, R. S. (1997). T promoter activity in the absence of functional T protein during axis formation and elongation in the mouse. *Dev Biol* **189**, 161-173.

Selleck, M. A. and Stern, C. D. (1991). Fate mapping and cell lineage analysis of Hensen's node in the chick embryo. *Development* **112**, 615-626.

Serizawa, T., Isotani, A., Matsumura, T., Nakanishi, K., Nonaka, S., Shibata, S., Ikawa, M. and Okano, H. (2019). Developmental analyses of mouse embryos and adults using a non-overlapping tracing system for all three germ layers. *Development* **146**.

Sharma, R., Shafer, M. E. R., Bareke, E., Tremblay, M., Majewski, J. and Bouchard, M. (2017). Bmp signaling maintains a mesoderm progenitor cell state in the mouse tailbud. *Development* **144**, 2982-2993.

Shields, D. C., Ramsbottom, D., Donoghue, C., Pinjon, E., Kirke, P. N., Molloy, A. M., Edwards, Y. H., Mills, J. L., Mynett-Johnson, L., Weir, D. G., et al. (2000). Association between historically high frequencies of neural tube defects and the human T homologue of mouse T (Brachyury). *Am J Med Genet* **92**, 206-211.

Shum, A. S., Poon, L. L., Tang, W. W., Koide, T., Chan, B. W., Leung, Y. C., Shiroishi, T. and Copp, A. J. (1999). Retinoic acid induces down-regulation of Wnt-3a, apoptosis and diversion of tail bud cells to a neural fate in the mouse embryo. *Mech Dev* **84**, 17-30.

Sirbu, I. O. and Duester, G. (2006). Retinoic-acid signalling in node ectoderm and posterior neural plate directs left-right patterning of somitic mesoderm. *Nat Cell Biol* **8**, 271-277.

Sonnen, K. F., Lauschke, V. M., Uraji, J., Falk, H. J., Petersen, Y., Funk, M. C., Beaupeux, M., Francois, P., Merten, C. A. and Aulehla, A. (2018). Modulation of Phase Shift between Wnt and Notch Signaling Oscillations Controls Mesoderm Segmentation. *Cell* **172**, 1079-1090 e1012.

Steventon, B., Duarte, F., Lagadec, R., Mazan, S., Nicolas, J. F. and Hirsinger, E. (2016). Species-specific contribution of volumetric growth and tissue convergence to posterior body elongation in vertebrates. *Development* **143**, 1732-1741.

Sudheer, S., Liu, J., Marks, M., Koch, F., Anurin, A., Scholze, M., Senft, A. D., Wittler, L., Macura, K., Grote, P., et al. (2016). Different Concentrations of FGF Ligands, FGF2 or FGF8 Determine Distinct States of WNT-Induced Presomitic Mesoderm. *Stem Cells* **34**, 1790-1800.

Szumska, D., Pieles, G., Essalmani, R., Bilski, M., Mesnard, D., Kaur, K., Franklyn, A., El Omari, K., Jefferis, J., Bentham, J., et al. (2008). VACTERL/caudal regression/Currarino syndrome-like malformations in mice with mutation in the proprotein convertase Pcsk5. *Genes Dev* **22**, 1465-1477.

Taguchi, A., Kaku, Y., Ohmori, T., Sharmin, S., Ogawa, M., Sasaki, H. and Nishinakamura, R. (2014). Redefining the In Vivo Origin of Metanephric Nephron Progenitors Enables Generation of Complex Kidney Structures from Pluripotent Stem Cells. *Cell Stem Cell* **14**, 53-67.

Taguchi, A. and Nishinakamura, R. (2017). Higher-Order Kidney Organogenesis from Pluripotent Stem Cells. *Cell Stem Cell* **21**, 730-+.

Tahara, N., Kawakami, H., Chen, K. Q., Anderson, A., Yamashita Peterson, M., Gong, W., Shah, P., Hayashi, S., Nishinakamura, R., Nakagawa, Y., et al. (2019). Sall4 regulates neuromesodermal progenitors and their descendants during body elongation in mouse embryos. *Development* **146**.

Takada, S., Stark, K. L., Shea, M. J., Vassileva, G., McMahon, J. A. and McMahon, A. P. (1994). Wnt-3a regulates somite and tailbud formation in the mouse embryo. *Genes Dev* **8**, 174-189.

Takasato, M., Er, P. X., Chiu, H. S., Maier, B., Baillie, G. J., Ferguson, C., Parton, R. G., Wolvetang, E. J., Roost, M. S., Lopes, S. M. C. D., et al. (2015). Kidney organoids from human iPS cells contain multiple lineages and model human nephrogenesis. *Nature* **526**, 564-U238.

Takemoto, T., Uchikawa, M., Kamachi, Y. and Kondoh, H. (2006). Convergence of Wnt and FGF signals in the genesis of posterior neural plate through activation of the Sox2 enhancer N-1. *Development* **133**, 297-306.

Takemoto, T., Uchikawa, M., Yoshida, M., Bell, D. M., Lovell-Badge, R., Papaioannou, V. E. and Kondoh, H. (2011). Tbx6-dependent Sox2 regulation determines neural or mesodermal fate in axial stem cells. *Nature* **470**, 394-398.

Tam, P. P. (1981). The control of somitogenesis in mouse embryos. *J Embryol Exp Morphol* **65 Suppl**, 103-128.

Tam, P. P. (1986). A study of the pattern of prospective somites in the presomitic mesoderm of mouse embryos. *J Embryol Exp Morphol* **92**, 269-285.

Tam, P. P. and Tan, S. S. (1992). The somitogenetic potential of cells in the primitive streak and the tail bud of the organogenesis-stage mouse embryo. *Development* **115**, 703-715.

Taniguchi, Y., Kurth, T., Weiche, S., Reichelt, S., Tazaki, A., Perike, S., Kappert, V. and Epperlein, H. H. (2017). The posterior neural plate in axolotl gives rise to neural tube or turns anteriorly to form somites of the tail and posterior trunk. *Dev Biol* **422**, 155-170.

Tsakiridis, A., Huang, Y., Blin, G., Skylaki, S., Wymeersch, F., Osorno, R., Economou, C., Karagianni, E., Zhao, S., Lowell, S., et al. (2014). Distinct Wnt-driven primitive streak-like populations reflect in vivo lineage precursors. *Development* **141**, 1209-1221.

Tsakiridis, A. and Wilson, V. (2015). Assessing the bipotency of in vitro-derived neuromesodermal progenitors. *F1000Res* **4**, 100.

Tucker, A. S. and Slack, J. M. (1995). Tail bud determination in the vertebrate embryo. *Curr Biol* **5**, 807-813.

Turner, D. A., Hayward, P. C., Baillie-Johnson, P., Rue, P., Broome, R., Faunes, F. and Martinez Arias, A. (2014). Wnt/beta-catenin and FGF signalling direct the specification and maintenance of a neuromesodermal axial progenitor in ensembles of mouse embryonic stem cells. *Development* **141**, 4243-4253.

Tzouanacou, E., Wegener, A., Wymeersch, F. J., Wilson, V. and Nicolas, J. F. (2009). Redefining the progression of lineage segregations during mammalian embryogenesis by clonal analysis. *Dev Cell* **17**, 365-376.

Ukita, K., Hirahara, S., Oshima, N., Imuta, Y., Yoshimoto, A., Jang, C. W., Oginuma, M., Saga, Y., Behringer, R. R., Kondoh, H., et al. (2009). Wnt signaling maintains the notochord fate for progenitor cells and supports the posterior extension of the notochord. *Mech Dev* **126**, 791-803.

van den Brink, S. C., Alemany, A., van Batenburg, V., Moris, N., Blotenburg, M., Vivie, J., Baillie-Johnson, P., Nichols, J., Sonnen, K. F., Martinez Arias, A., et al. (2020). Single-cell and spatial transcriptomics reveal somitogenesis in gastruloids. *Nature*.

van Rooijen, C., Simmini, S., Bialecka, M., Neijts, R., van de Ven, C., Beck, F. and Deschamps, J. (2012). Evolutionarily conserved requirement of Cdx for post-occipital tissue emergence. *Development* **139**, 2576-2583.

Veenvliet, J. S., Bolondi, A., Kretzmer, H., Haut, L., Scholze-Wittler, M., Schifferl, D., Koch, F., Pustet, M., Heimann, S., Buschow, R., Wittler, L., Timmermann, B., Meissner, A., and Herrmann, B.G. (2020). Mouse embryonic stem cells self-organize into trunklike structures with neural tube and somites. *bioRxiv*.

Vega-Lopez, G. A., Cerrizuela, S., Tribulo, C. and Aybar, M. J. (2018). Neurocristopathies: New insights 150 years after the neural crest discovery. *Dev Biol* **444 Suppl 1**, S110-S143.

Verrier, L., Davidson, L., Gierlinski, M., Dady, A. and Storey, K. G. (2018). Neural differentiation, selection and transcriptomic profiling of human neuromesodermal progenitor-like cells in vitro. *Development* **145**.

Wacker, S. A., Jansen, H. J., McNulty, C. L., Houtzager, E. and Durston, A. J. (2004). Timed interactions between the Hox expressing non-organiser mesoderm and the Spemann organiser generate positional information during vertebrate gastrulation. *Dev Biol* **268**, 207-219.

West, C. M. (1937). A Human Embryo of Twenty-five Somites. *J Anat* **71**, 169-200 161.

White, P. H., Farkas, D. R. and Chapman, D. L. (2005). Regulation of Tbx6 expression by Notch signaling. *Genesis* **42**, 61-70.

Wilson, V. and Beddington, R. S. (1996). Cell fate and morphogenetic movement in the late mouse primitive streak. *Mech Dev* **55**, 79-89.

Wilson, V., Manson, L., Skarnes, W. C. and Beddington, R. S. (1995). The T gene is necessary for normal mesodermal morphogenetic cell movements during gastrulation. *Development* **121**, 877-886.

Wilson, V., Olivera-Martinez, I. and Storey, K. G. (2009). Stem cells, signals and vertebrate body axis extension. *Development* **136**, 1591-1604.

Wind, M., Gogolou, A., Manipur, I., Granata, G., Butler, L., Andrews, P. W., Barbaric, I., Ning, K., Guarracino, G. M., Placzek, M. and Tsakiridis, A. (2020). Defining the signalling determinants of a posterior ventral spinal cord identity in human neuromesodermal progenitor derivatives. *bioRxiv*.

Wood, T. R., Kyrsting, A., Stegmaier, J., Kucinski, I., Kaminski, C.F., Mikut, R., and Voiculescu, O. (2019). Neuromesodermal progenitors separate the axial stem zones while producing few single- and dual-fated descendants. *bioRiv*.

Wymeersch, F. J., Huang, Y., Blin, G., Cambray, N., Wilkie, R., Wong, F. C. and Wilson, V. (2016). Position-dependent plasticity of distinct progenitor types in the primitive streak. *Elife* **5**, e10042.

Wymeersch, F. J., Skylaki, S., Huang, Y., Watson, J. A., Economou, C., Marek-Johnston, C., Tomlinson, S. R. and Wilson, V. (2019). Transcriptionally dynamic progenitor populations organised around a stable niche drive axial patterning. *Development* **146**.

Xi, H., Fujiwara, W., Gonzalez, K., Jan, M., Liebscher, S., Van Handel, B., Schenke-Layland, K. and Pyle, A. D. (2017). In Vivo Human Somitogenesis Guides Somite Development from hPSCs. *Cell Rep* **18**, 1573-1585.

Yamaguchi, T. P., Takada, S., Yoshikawa, Y., Wu, N. and McMahon, A. P. (1999). T (Brachyury) is a direct target of Wnt3a during paraxial mesoderm specification. *Genes Dev* **13**, 3185-3190.

Yasuhiko, Y., Haraguchi, S., Kitajima, S., Takahashi, Y., Kanno, J. and Saga, Y. (2006). Tbx6-mediated Notch signaling controls somite-specific Mesp2 expression. *Proc Natl Acad Sci U S A* **103**, 3651-3656.

Yoshikawa, Y., Fujimori, T., McMahon, A. P. and Takada, S. (1997). Evidence that absence of Wnt-3a signaling promotes neuralization instead of paraxial mesoderm development in the mouse. *Dev Biol* **183**, 234-242.

Young, T., Rowland, J. E., van de Ven, C., Bialecka, M., Novoa, A., Carapuco, M., van Nes, J., de Graaff, W., Duluc, I., Freund, J. N., et al. (2009). Cdx and Hox genes differentially regulate posterior axial growth in mammalian embryos. *Dev Cell* **17**, 516-526.

Zhao, T., Gan, Q., Stokes, A., Lassiter, R. N., Wang, Y., Chan, J., Han, J. X., Pleasure, D. E., Epstein, J. A. and Zhou, C. J. (2014). beta-catenin regulates Pax3 and Cdx2 for caudal neural tube closure and elongation. *Development* **141**, 148-157.

Tables

Table 1. Key transcription factors controlling NMP cell fate decisions

Gene	Role	References
Brachyury (*T*)	Mesoderm exit from primitive streak; paraxial mesoderm differentiation; inhibition of neural differentiation; Wnt/Fgf signalling stimulation; RA signalling antagonism.	Amin et al., 2016; Gentsch et al., 2013; Gouti et al., 2014; Koch et al., 2017; Lolas et al., 2014; Martin and Kimelman, 2008; Martin and Kimelman, 2010; Rashbass et al., 1994; Wilson et al., 1995; Yamaguchi et al., 1999
Cdx	Wnt/Fgf signalling stimulation; paraxial mesoderm differentiation; trunk Hox gene activation; RA signalling antagonism.	Amin et al., 2016; Gouti et al., 2017; Metzis et al., 2018; Savory et al., 2009; van Rooijen et al., 2012; Young et al., 2009
Trunk *Hox* (*Hoxa5*, *Hoxb8*)	Wnt signalling stimulation; RA signalling antagonism.	Young et al., 2009

Hox(a-c)13	*Cdx* antagonism; RA signalling stimulation; *T*/Wnt/Fgf signalling antagonism; proliferation/apoptosis control in tailbud; Lin28 repression.	Aires et al., 2019; Amin et al., 2016; Denans et al., 2015; Economides et al., 2003; Young et al., 2009
Oct4	Posterior Hox gene antagonism; paraxial mesoderm/posterior neurectoderm differentiation; proliferation; maintenance of adhesion.	Aires et al., 2016; DeVeale et al., 2013; Economou et al., 2015; Livigni et al., 2013
Sall4	NMP generation; paraxial mesoderm/posterior neurectoderm differentiation; Wnt signalling stimulation.	Tahara et al., 2019
cMyc	Mesoderm/posterior neurectoderm differentiation; Wnt/Fgf signalling stimulation (*in vitro*/explants).	Mastromina et al., 2018
Tet1/2/3	Paraxial mesoderm/posterior neurectoderm differentiation; Wnt signalling antagonism.	Li et al., 2016
Lin28a	Paraxial mesoderm differentiation; inhibition of neural differentiation; Wnt/Fgf signalling stimulation; proliferation.	Robinton et al., 2019
Tbx6	Paraxial mesoderm differentiation/EMT; inhibition of neural differentiation.	Bouldin et al., 2015; Goto et al., 2017; Javali et al., 2017; Koch et al., 2017; Takemoto et al., 2011
Msgn1	Paraxial mesoderm differentiation.	Chalamalasetty et al., 2014; Gouti et al., 2017
Med12	Paraxial mesoderm differentiation; WNT and WNT/PCP signalling stimulation.	Rocha et al., 2010

Table 2. Key signalling pathway components controlling NMP cell fate decisions

Signalling pathway	**Signalling component**	**Role**	**References**

Wnt	*Wnt8c*	Control of posterior *Sox2* expression via N-1 enhancer; inhibition of neural differentiation.	Olivera-Martinez and Storey, 2007; Takemoto et al., 2006
	Wnt8a	Anterior paraxial mesoderm differentiation (together with *Wnt3a*); inhibition of neural differentiation; induction of Fgf signalling.	Cunningham et al., 2015
	Wnt3a	Induction of posterior Hox/*Cdx* expression in neural cells; paraxial mesoderm (high levels)/posterior neurectoderm (low levels) differentiation; induction of Fgf signalling; inhibition of neural differentiation; NMP maintenance.	Cunningham et al., 2015; Garriock et al., 2015; Jurberg et al., 2014; Nordstrom et al., 2006; Yoshikawa et al., 1997
	Ctnnb1	Paraxial mesoderm/posterior neurectoderm differentiation; NMP maintenance.	Dunty et al., 2008; Garriock et al., 2015; Wymeersch et al., 2016
	Sp5. Sp8, Axin2, Tcf1, Lef1	Wnt effectors; paraxial mesoderm differentiation.	Dunty et al., 2014; Galceran et al., 1999; Kennedy et al., 2016; Qian et al., 2011
	Wnt3	Control of posterior *Sox2* expression via N1 enhancer.	Takemoto et al., 2006
Wnt/planar cell polarity (PCP)	*Vangl2*	Posterior neurectoderm differentiation.	Lopez-Escobar et al., 2018
	Wnt5a, Wnt11	Paraxial mesoderm differentiation; EMT, proliferation.	Andre et al., 2015
Fibroblast growth factor (Fgf)	*Fgf8*	Control of posterior *Sox2* expression via N1 enhancer; paraxial mesoderm differentiation; NMP/neural progenitor maintenance; inhibition of definitive neural commitment; induction of Wnt signalling; RA signalling antagonism.	Boulet and Capecchi, 2012; Delfino-Machin et al., 2005; Diez del Corral et al., 2002; Diez del Corral et al., 2003; Olivera-Martinez et al., 2012; Olivera-Martinez and Storey, 2007; Takemoto et al., 2006
	Fgf4	Induction of posterior *Hox*/*Cdx* expression in neural cells;	Anderson, 2020; Boulet and Capecchi, 2012; Nordstrom et al., 2006

		paraxial mesoderm/posterior neurectoderm differentiation; induction of Wnt signalling; RA signalling antagonism.	
	Fgfr1	Paraxial mesoderm differentiation/EMT.	Goto et al., 2017
Retinoic acid (RA)	*Raldh2, RARβ, Aldh1a2*	Posterior neurectoderm differentiation; Fgf signalling antagonism; inhibition of mesoderm differentiation; NMP induction (low levels of RA); neurectoderm proliferation.	Diez del Corral et al., 2003; Gouti et al., 2017; Kumar and Duester, 2014; Molotkova et al., 2005; Olivera-Martinez et al., 2012; Ribes et al., 2009
Notch	*Delta1*	Posterior neurectoderm differentiation.	Akai et al., 2005
	RBP-Jκ	Paraxial mesoderm differentiation.	White et al., 2005
Transforming growth factor β (Tgfβ)	*Gfd8, Gdf11*	Trunk-to-tail transition; RA signalling antagonism; tailbud NMP maintenance; activation of Hox13 genes; Lin28 repression.	Aires et al., 2019; Jurberg et al., 2013
	TgfβRI	Trunk-to-tail transition; tail bud EMT control.	Dias et al., 2020
	Bmp4	Paraxial mesoderm differentiation in tailbud; control of LPMP fate.	Row et al., 2018; Sharma et al., 2017

EMT, epithelial-mesenchymal transition; LPMP, lateral and paraxial mesoderm progenitors; NMP, neuromesodermal progenitor.

Table 3. Published studies reporting the *in vitro* generation of NMP-like cells

Study	**PSC Source**	**Signals**	**Basal medium/coating substrates**	**Duration(days)**	**%T^+SOX2^+ cells**	**Differentiation potential**
Tsakiridis et al. 2014	mEpiSCs	CHIR; FGF2; Activin A	N2B27/Fibronectin	2	~10–15%	Posterior neural; Paraxial mesoderm and lateral plate-ventral mesoderm[2]
(i) Gouti et al. 2014;	mESCs	FGF2 (d1-3); CHIR (d 2-3)	N2B27/CellBIND, Surface-Gelatin	3	~80%	Posterior neural and

(ii) Cunningham et al. 2016; (iii) de Lemos et al. 2019						paraxial mesoderm[1,2]; lateral plate mesoderm[1]
(i) Gouti et al. 2014; (ii) Tsakiridis and Wilson 2015; (iii) Row et al. 2018; (iv) Edri et al. 2019	mEpiSC	FGF2; CHIR	N2B27/Fibronectin	2–3	~50–80%	Posterior neural and paraxial mesoderm[1,2]; lateral plate mesoderm[1]
Gouti et al. 2014	hPSCs	FGF2; CHIR; ROCKi (d0–1)	N2B27/Fibronectin	2–4	~60–80%	Posterior neural and paraxial mesoderm[1]
Turner et al. 2014	mESCs	FGF2 (d2-3); CHIR (d2-3)	N2B27/Gelatin	3	n.d.	n.d., but evidence of A-P regionalisation
Lippmann et al. 2015	hPSCs	FGF8b(after d1); CHIR (after d2); ROCKi (d0–2)	E6/Vitronectin	3–7	~75-100%	Posterior neural[1]
Denham et al. 2015	hPSCs	CHIR; SB43	N2B27/Laminin	4	~97%	Posterior neural and neural crest[1]
Amin et al. 2016	mEpiSCs	FGF8; CHIR or WNT3A	N2B27/Fibronectin	1	n.d.	n.d.
Verrier et al. 2018	hPSCs	FGF2; CHIR; SB43; NOG (d2–3)	N2B27/Geltrex	3	n.d.	Posterior neural[1]
Kumamaru et al. 2018	hPSCs	FGF2; FGF8; CHIR; SB43; LDN;	N2B27/Matrigel	3	n.d.	Posterior neural and self-renewing neural stem cells[1]

		DAPT				
Frith et al. 2018	hPSCs	FGF2; CHIR	N2B27/Vitronectin	2–3	~80%	Posterior neural, Paraxial mesoderm and neural Crest[1]
Kirino et al. 2018	hPSCs	CHIR; SB43	E6/Floating culture on ultra-low attachment plates	3	n.d.	Posterior neural and neural crest[1]
Edri et al. 2019	mEpiSCs	FGF2; Activin A (d0-1); CHIR (d2-3)	N2B27/Fibronectin	3	n.d.	Posterior neural and paraxial mesoderm[1,2]; lateral plate mesoderm[1]
Hackland et al. 2019	hPSCs	CHIR; ROCKi	N2/DMEM-F12/Matrigel	2	~50-80%	Paraxial mesoderm and neural crest[1]
Diaz-Cuadros et al. 2020	hPSCs	CHIR LDN	DMEM-F12/Geltrex	1	n.d.	Paraxial mesoderm[1]
Cooper et al. 2020	hPSCs	FGF2 CHIR AGN ROCKi	N2B27 (minus vitamin A)/Vitronectin	1.5	n.d.	Posterior neural and neural crest[1]

AGN, AGN193109; CHIR, CHIR 99021; d, day; E6, DAPT; E6; Essential 6; hPSCs, human pluripotent stem cells; LDN, LDN193189; mEpiSCs, mouse Epiblast stem cells; n.d., not determined; NOG, Noggin; ROCKi, ROCK inhibition; SB43, SB 431542.

[1] *in vitro* marker analysis

[2] engraftment into embryo.

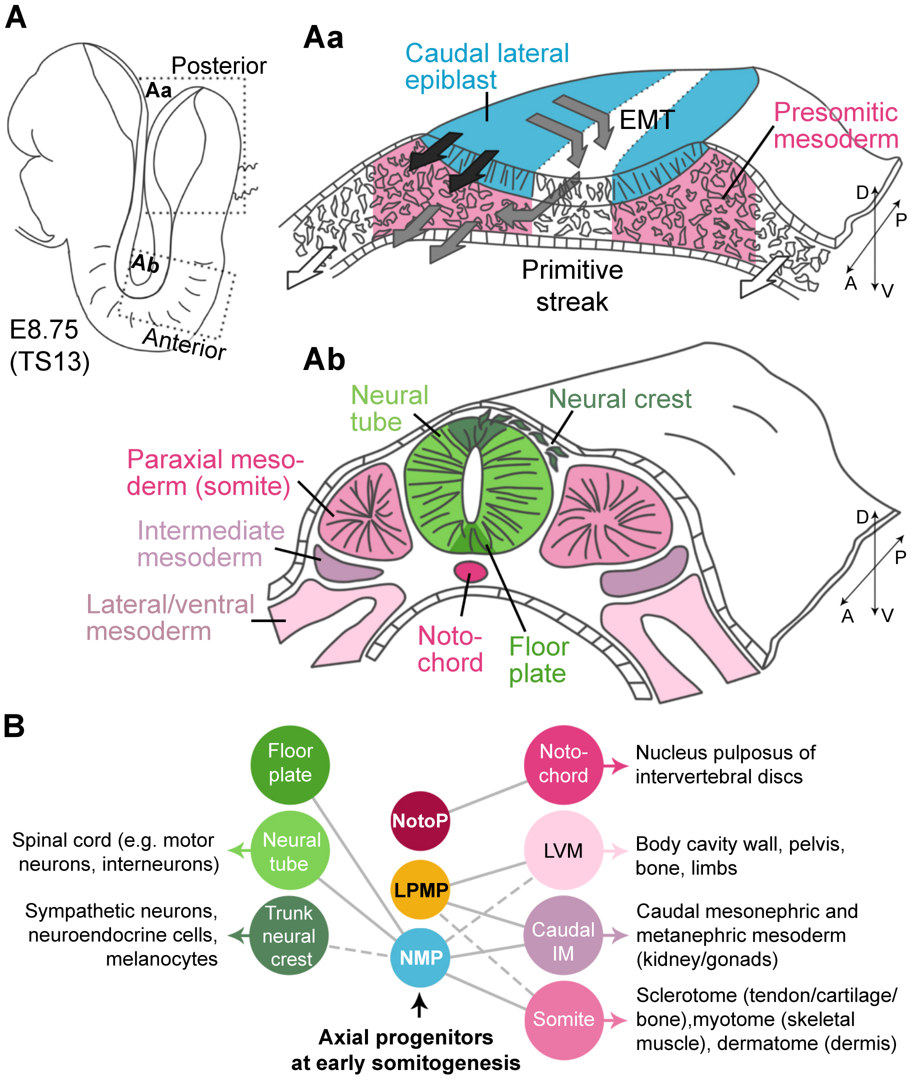
A
Posterior
Aa
Ab
E8.75
(TS13)
Anterior
Aa
Caudal lateral
epiblast
EMT
Presomitic
mesoderm
Primitive
streak
D
P
A
V
Ab
Neural
tube
Neural crest
Paraxial meso-
derm (somite)
Intermediate
mesoderm
Lateral/ventral
mesoderm
Noto-
chord
Floor
plate
D
P
A
V
B
Floor
plate
Noto-
chord
Nucleus pulposus of
intervertebral discs
NotoP
Spinal cord (e.g. motor
neurons, interneurons)
Neural
tube
LVM
Body cavity wall, pelvis,
bone, limbs
LPMP
Sympathetic neurons,
neuroendocrine cells,
melanocytes
Trunk
neural
crest
Caudal
IM
Caudal mesonephric and
metanephric mesoderm
(kidney/gonads)
NMP
Somite
Sclerotome (tendon/cartilage/
bone),myotome (skeletal
muscle), dermatome (dermis)
Axial progenitors
at early somitogenesis

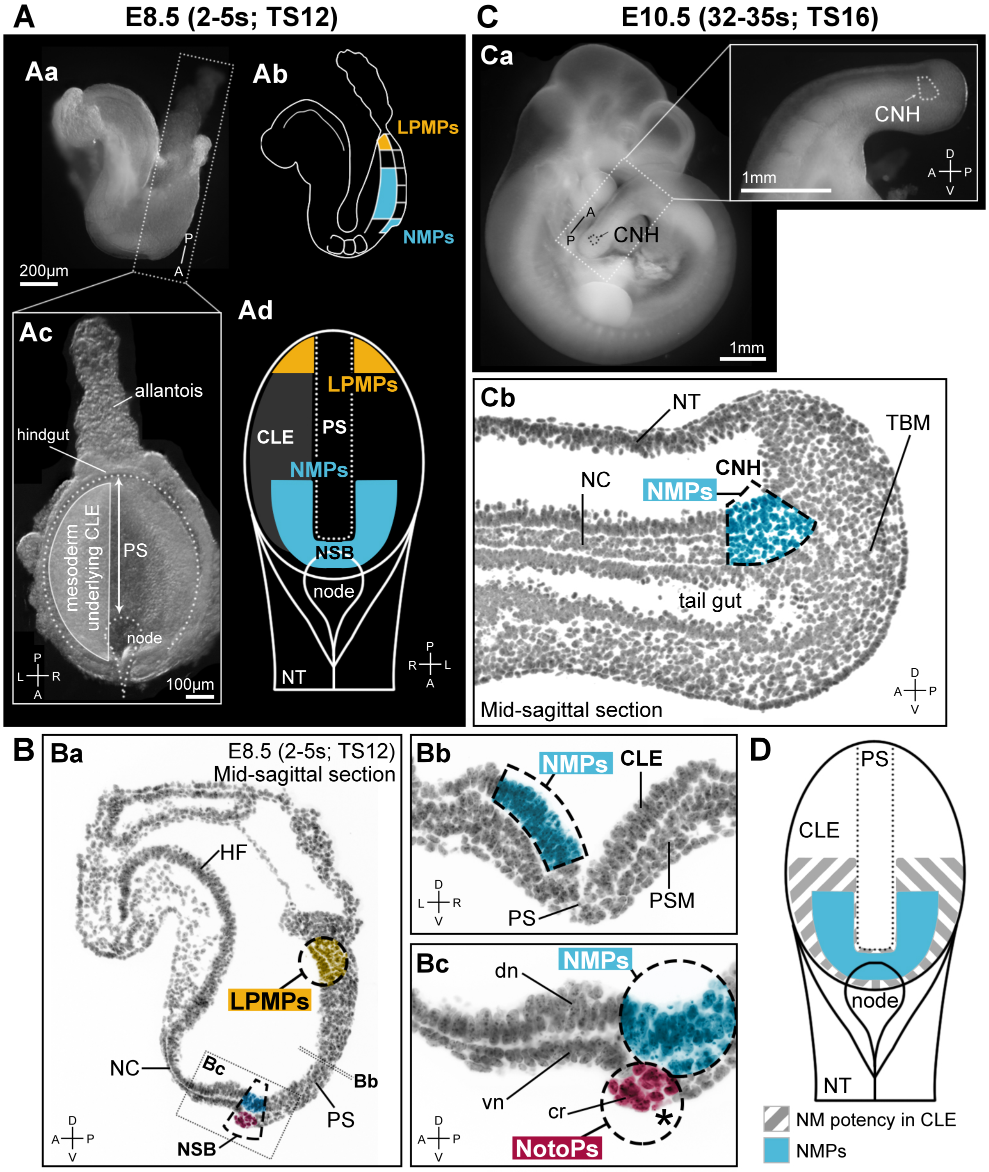
A
E8.5 (2-5s; TS12)
Aa
P
A
200µm
Ab
LPMPs
NMPs
Ac
allantois
hindgut
mesoderm underlying CLE
PS
node
P
L
R
A
100µm
Ad
LPMPs
PS
CLE
NMPs
NSB
node
NT
P
R
L
A
C
E10.5 (32-35s; TS16)
Ca
CNH
1mm
D
A
P
V
A
P
CNH
1mm
Cb
NT
TBM
NC
CNH
NMPs
tail gut
Mid-sagittal section
D
A
P
V
B
Ba
E8.5 (2-5s; TS12)
Mid-sagittal section
HF
LPMPs
NC
Bc
Bb
PS
NSB
D
A
P
V
Bb
NMPs
CLE
PSM
PS
D
L
R
V
Bc
dn
NMPs
vn
cr
*
NotoPs
D
A
P
V
D
PS
CLE
node
NT
NM potency in CLE
NMPs

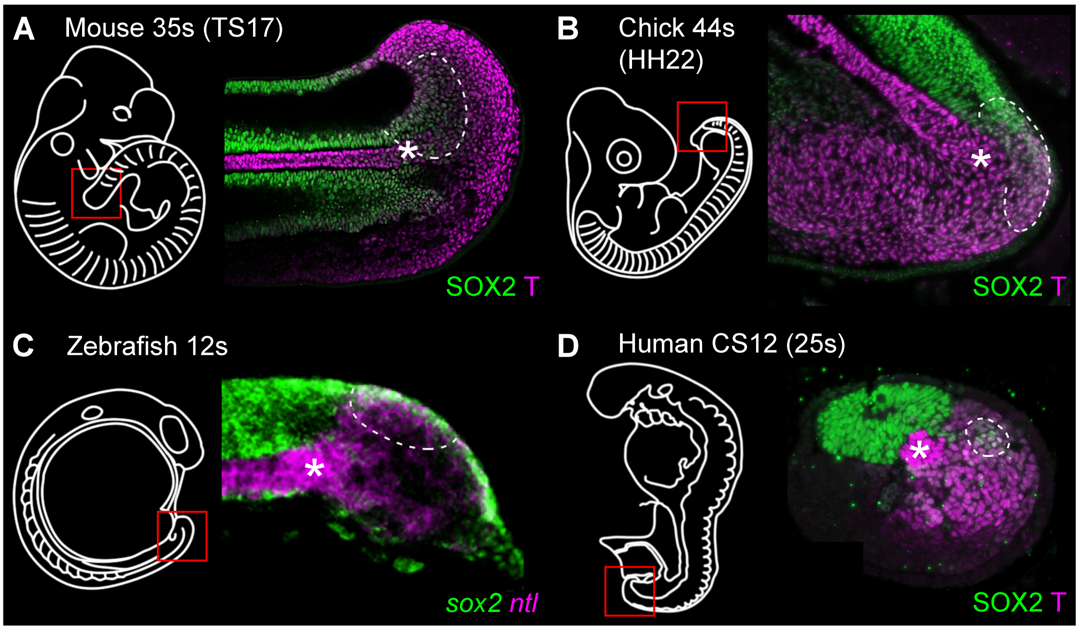
A
Mouse 35s (TS17)
*
SOX2 T
B
Chick 44s
(HH22)
*
SOX2 T
C
Zebrafish 12s
*
sox2 ntl
D
Human CS12 (25s)
*
SOX2 T

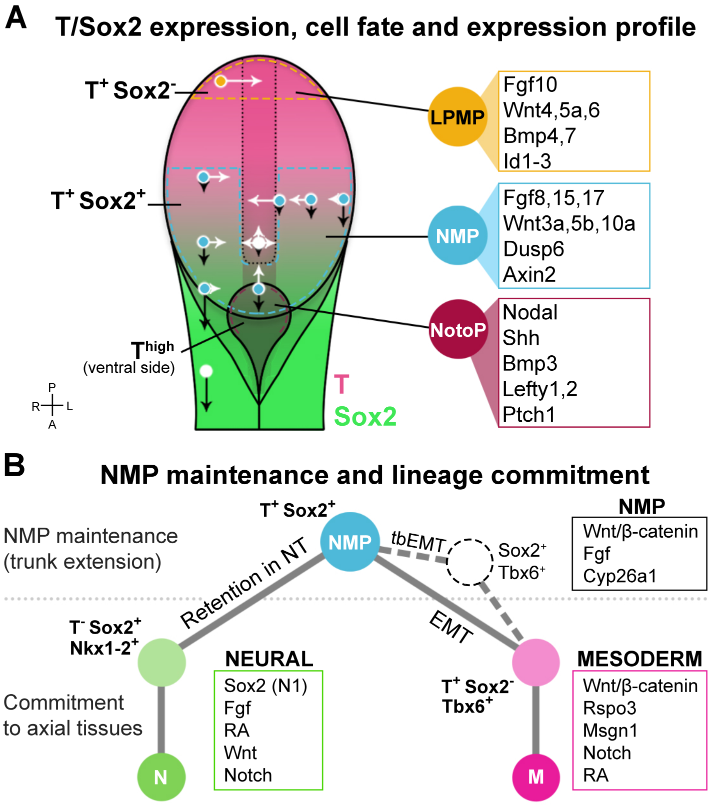
A
T/Sox2 expression, cell fate and expression profile
T+ Sox2-
T+ Sox2+
Thigh
(ventral side)
P
R
L
A
T
Sox2
LPMP
Fgf10
Wnt4,5a,6
Bmp4,7
Id1-3
NMP
Fgf8,15,17
Wnt3a,5b,10a
Dusp6
Axin2
NotoP
Nodal
Shh
Bmp3
Lefty1,2
Ptch1
B
NMP maintenance and lineage commitment
T+ Sox2+
NMP
NMP maintenance
(trunk extension)
Retention in NT
tbEMT
Sox2+
Tbx6+
EMT
NMP
Wnt/β-catenin
Fgf
Cyp26a1
T- Sox2+
Nkx1-2+
NEURAL
Sox2 (N1)
Fgf
RA
Wnt
Notch
Commitment
to axial tissues
N
T+ Sox2-
Tbx6+
MESODERM
Wnt/β-catenin
Rspo3
Msgn1
Notch
RA
M

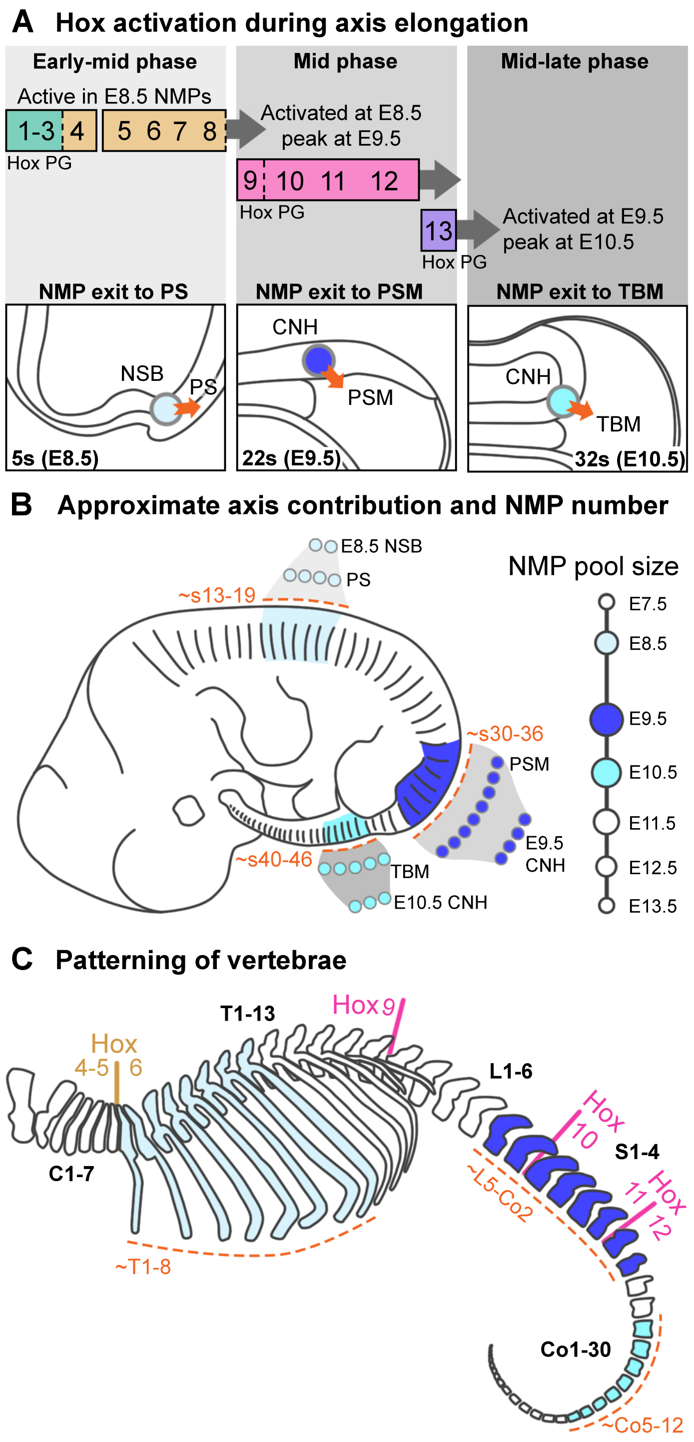
A Hox activation during axis elongation
Early-mid phase
Active in E8.5 NMPs
1-3
4
5 6 7 8
Hox PG
Mid phase
Activated at E8.5
peak at E9.5
9
10 11 12
Hox PG
Mid-late phase
13
Hox PG
Activated at E9.5
peak at E10.5
NMP exit to PS
NSB
PS
5s (E8.5)
NMP exit to PSM
CNH
PSM
22s (E9.5)
NMP exit to TBM
CNH
TBM
32s (E10.5)
B Approximate axis contribution and NMP number
E8.5 NSB
PS
~s13-19
~s30-36
PSM
E9.5
CNH
~s40-46
TBM
E10.5 CNH
NMP pool size
E7.5
E8.5
E9.5
E10.5
E11.5
E12.5
E13.5
C Patterning of vertebrae
Hox
4-5
6
T1-13
Hox 9
C1-7
~T1-8
L1-6
Hox
10
S1-4
Hox
11
12
~L5-Co2
Co1-30
~Co5-12

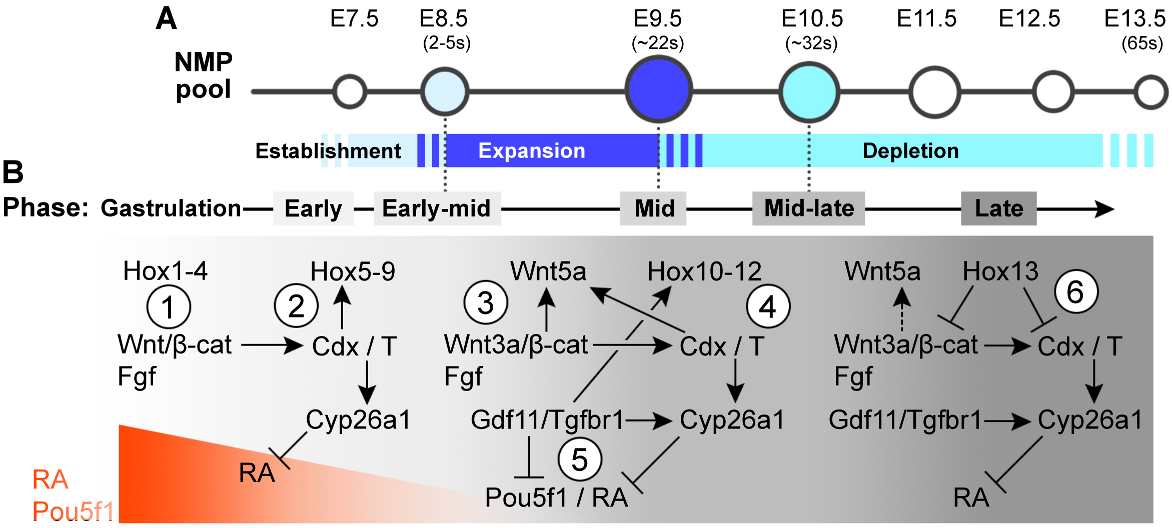
A
NMP pool
E7.5
E8.5
(2-5s)
E9.5
(~22s)
E10.5
(~32s)
E11.5
E12.5
E13.5
(65s)
Establishment
Expansion
Depletion
B
Phase: Gastrulation
Early
Early-mid
Mid
Mid-late
Late
Hox1-4
①
Wnt/β-cat
Fgf
Hox5-9
②
Cdx / T
Cyp26a1
RA
RA
Pou5f1
Wnt5a
③
Wnt3a/β-cat
Fgf
Hox10-12
④
Cdx / T
Gdf11/Tgfbr1
Cyp26a1
⑤
Pou5f1 / RA
Wnt5a
Hox13
⑥
Wnt3a/β-cat
Fgf
Cdx / T
Gdf11/Tgfbr1
Cyp26a1
RA

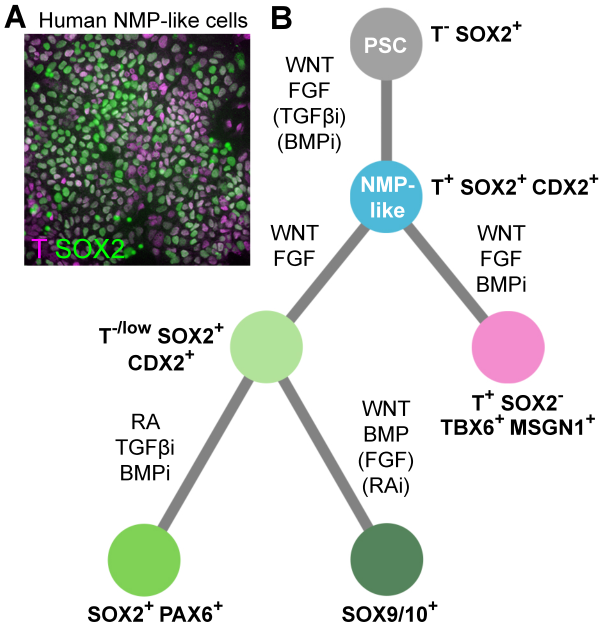
A
Human NMP-like cells
T SOX2
B
PSC
T$^-$ SOX2$^+$
WNT
FGF
(TGFβi)
(BMPi)
NMP-like
T$^+$ SOX2$^+$ CDX2$^+$
WNT
FGF
WNT
FGF
BMPi
T$^{-/low}$ SOX2$^+$ CDX2$^+$
T$^+$ SOX2$^-$ TBX6$^+$ MSGN1$^+$
RA
TGFβi
BMPi
WNT
BMP
(FGF)
(RAi)
SOX2$^+$ PAX6$^+$
SOX9/10$^+$